



Synsedimentary glacetectonic deformation within a glacialacustrine-esker sequence, Teesdale, Northern England

Emrys Phillips^{a,*}, David J.A. Evans^b

^a British Geological Survey, The Lyell Centre, Research Avenue South, Edinburgh, EH14 4AP, UK

^b Department of Geography, Durham University, South Road, Durham, DH1 3LE, UK

ARTICLE INFO

Article history:

Received 7 June 2019

Received in revised form 8 August 2019

Accepted 8 August 2019

Available online 31 August 2019

Keywords:

Glacetectonism

Microstructural analysis

Teesdale

County Durham

ABSTRACT

In glacial sedimentology there has been a recent improvement in the understanding of both progressive and polyphase deformation of glacial sequences, and the role played by water during these complex deformation histories. However, the processes occurring during the detachment and transport of sediment blocks during ice-marginal glacetectonic thrusting remain poorly understood. This lack of understanding is addressed in detail through a macro- and microscale study of the deformation structures in the glacial sequence exposed at Hayberries, Teesdale, County Durham (UK), where esker sands and gravels and associated tills truncate and overlie a sequence of rhythmically bedded glacialacustrine sands, silts and clays. Thrusts within the glacialacustrine and glacialfluvial sediments appear to be relatively sharp, planar structures. However, orientated thin sections reveal that these bedding-parallel detachments are marked by a thin layer of massive to foliated sand. The geometry of both meso and small-scale folds and sense of displacement on the thrusts is consistent with both brittle and ductile structures having formed in response to ice-push from the N/NW. Detailed analysis of the thin sections reveals that initial folding and thrusting was followed by the liquefaction and injection of a massive, matrix poor sand along the propagating thrust. Evidence for liquefaction and injection (sand-filled veins) increases towards the NW consistent with fluid flow and sediment injection accompanying SE-directed ice-push. These results suggest that the introduction of pressurised meltwater and sediment along the thrusts during deformation may facilitate decoupling and displacement along these detachments by thrust gliding.

© 2019 Published by Elsevier Ltd on behalf of The Geologists' Association.

1. Introduction

Micromorphological and microstructural analysis is a proven and well-established technique in geological structural and metamorphic studies, providing a wealth of data on the geometry and kinematics of deformation (see Passchier and Trouw, 1996; Phillips et al., 2011a,b, and references therein). In glacial sedimentology it is increasingly being used as a principal tool for distinguishing between subglacial and proglacial deformation, in particular the deformation histories recorded by the diamictos deposited in these two settings (van der Meer and Laban, 1990; van der Meer et al., 1992; van der Meer and Verbers, 1994; van der Meer, 1987, 1993; Menzies, 2000; Phillips and Auton, 2000; van der Wateren et al., 2000; Khatwa and Tulaczyk, 2001; Hart and Rose, 2001; Hiemstra and Rijdsdijk, 2003; van der Meer et al., 2003; Menzies et al., 2006; Phillips et al., 2007, 2011a,b, 2013a, 2018a,b;

Vaughan-Hirsch et al., 2013; Brumme, 2015; Gehrmann et al., 2017; Evans, 2018). Additionally, the detailed analysis of thin sections is being used with increasing success to aid our understanding of both progressive and polyphase deformation of glacial sequences (e.g. van der Wateren, 1995; Phillips and Auton, 2000; van der Wateren et al., 2000) as well as the role played by water during deformation (Hiemstra and van der Meer, 1997; Rijdsdijk et al., 1999; van der Meer et al., 1999; Phillips and Auton, 2000; Khatwa and Tulaczyk, 2001; Baroni and Fasano, 2006; Phillips and Merritt, 2008; van der Meer et al., 2009; Phillips et al., 2013b, 2018a,b). Hence, when used in combination with macroscale analysis, micromorphology enables the reconstruction of the complexities of glacial sedimentation and associated deformation events at key stratigraphic locations.

A complex sequence of glacialacustrine, glacialfluvial and till deposits in upper Teesdale, County Durham, has been analysed using macro- and microscale sedimentological techniques in order to decipher the nature and sequence of stillstands/readvances of the margins of the regional ice streams that covered the North Pennines during the last (Devensian) glacial stage. The sequence is

* Corresponding author.

E-mail address: erp@bgs.ac.uk (E. Phillips).

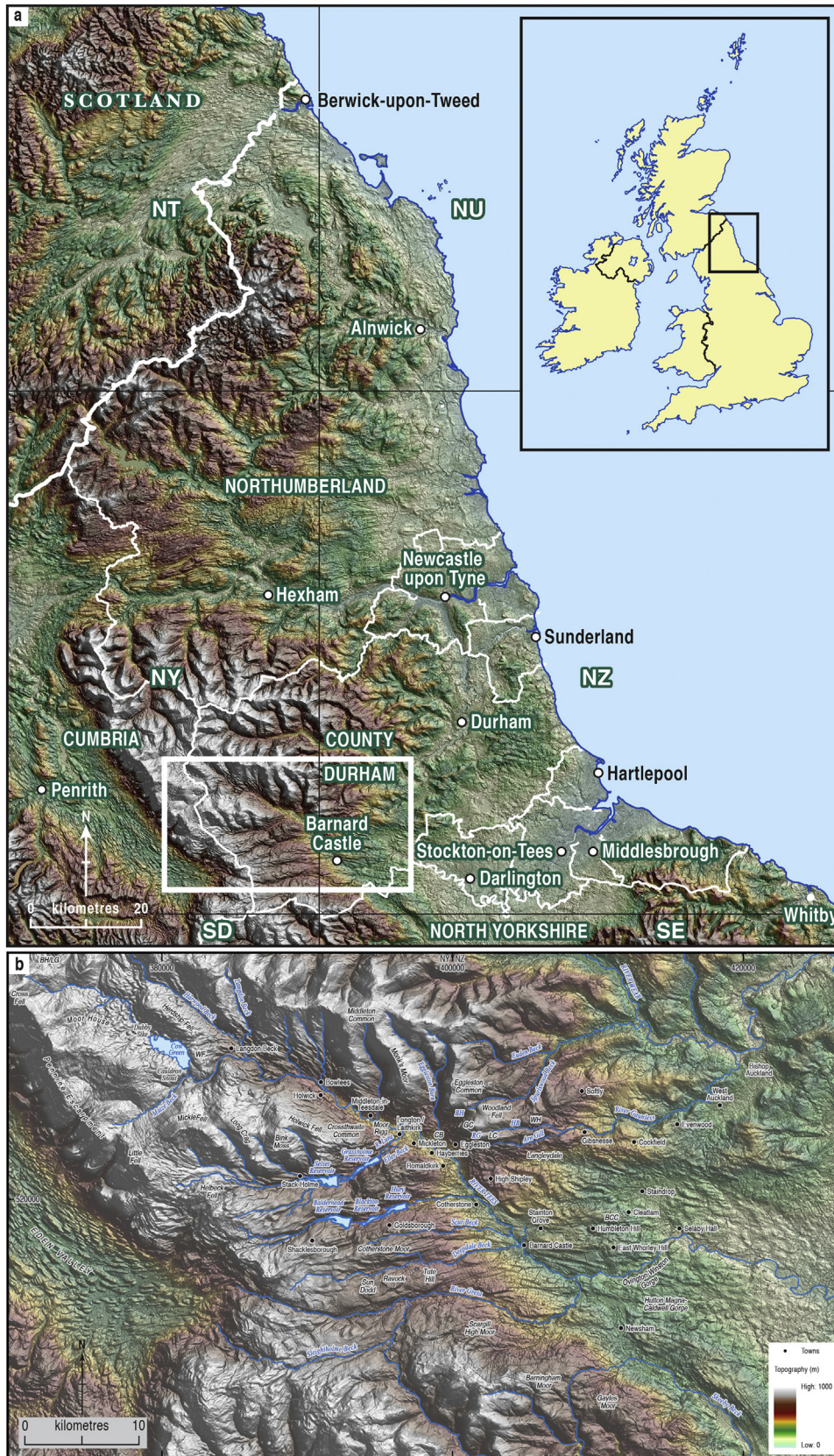


Fig. 1. Location maps and regional NEXTMap digital elevation model showing the location of Hayberries Quarry within the North Pennines uplands of Northern England. NEXTMap Britain elevation data from Intermap Technologies.

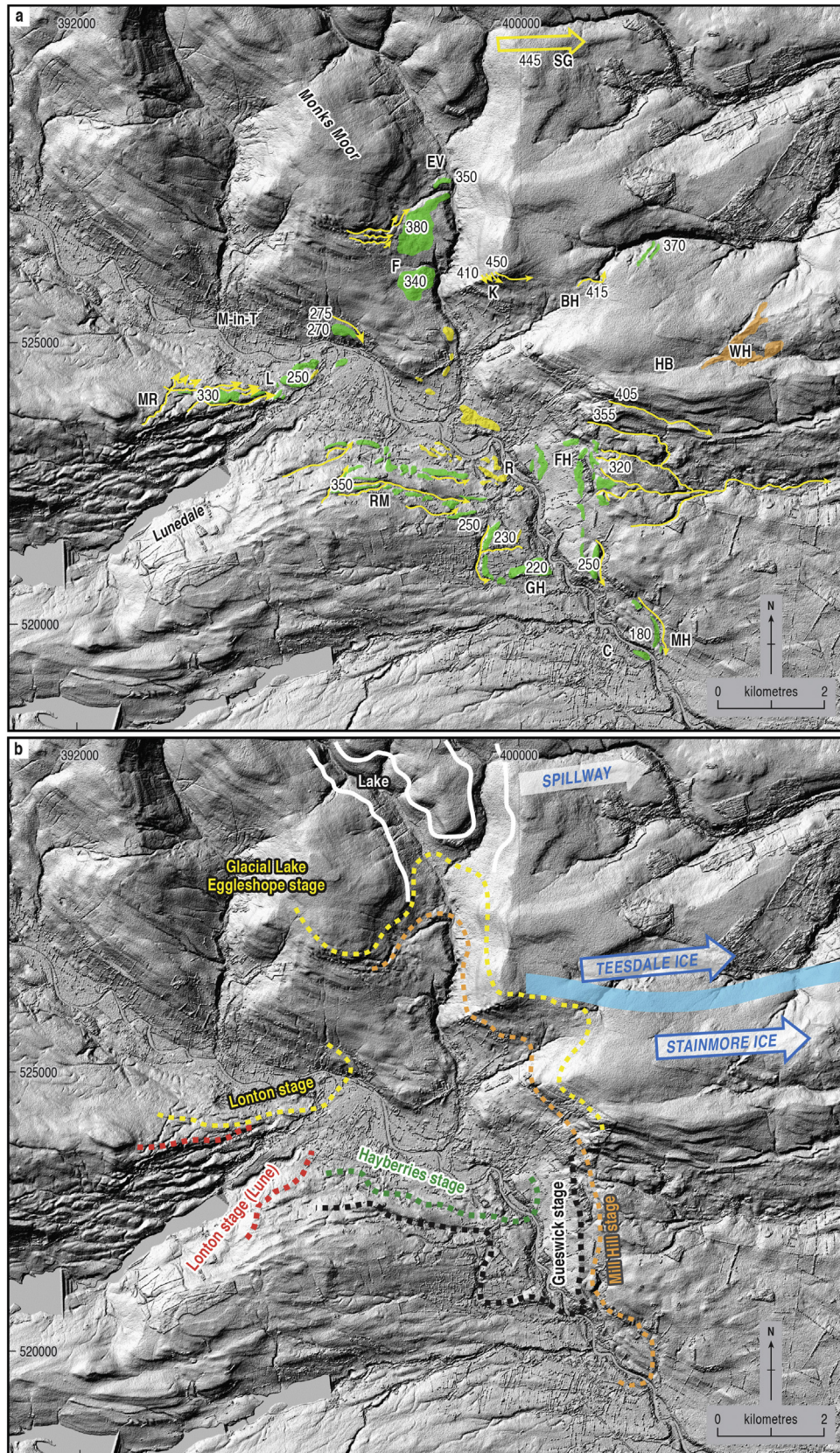


Fig. 2. Local NEXTMap digital elevation model covering the junction of upper Teesdale and the Stainmore Gap showing: (a) glacial geomorphology map; and (b) resulting ice marginal reconstructions for the Teesdale and Stainmore ice streams during the later stages of their recession in the North Pennine (Durham) dales (after Evans et al., 2018a). Symbols in (a) are as follows: green areas are glacial drift mounds and ridges, orange areas are glacial fluvial mounds interpreted either as eskers or kames, and yellow arrows represent selected relict (meltwater) channels associated with the drift mounds and ridges. Locations are: EV = Egglesthorpe Valley; SG with open yellow arrow = Sharnberry

exposed in a quarry at Hayberries, between the villages of Romalldkirk and Mickleton, 5.5 km east of Middleton-in-Teesdale (Fig. 1), and is a key stratigraphic location in the reconstruction of the oscillating margins of the local Teesdale glacier, nourished by North Pennines plateau icefields, and the regional Stainmore Ice Stream, driven by ice flow across the North Pennines watershed by Lake District and Scottish ice sources. Until recently very little was known about the nature of the suture zone between these ice streams or the pattern of their recession during Devensian (Dimlington Stadial) deglaciation. The Hayberries deposits have been critical to the identification of several phases of ice-marginal sedimentation (Evans et al., 2017, 2018a; Fig. 2), the details of which, more specifically, provide evidence of the relatively poorly understood processes operating during the detachment and transport of sediment blocks due to glactectonic disturbance. This study also demonstrates the value of a combined macro- and microscale approach to deciphering glacial depositional environments and thereby facilitating palaeoglaciological reconstructions.

2. Methods

Prior to sampling for micromorphology, the sedimentary sequence at Hayberries was logged and the macroscale characteristics, such as lithofacies classifications and architecture and macroscopic deformation structures, were described and sketched in detail, following the procedures prescribed in Evans and Benn (2004), Phillips et al. (2011a,b) and Evans (2018). Clast macrofabrics were measured from diamictons using 50 clasts per sample where possible, with a minimum of 30 clasts being necessary in sedimentary units where clasts were more sparsely distributed or to ensure that data collection was confined to small areas that reflected local variability in sediment properties (c.f., Evans and Hiemstra, 2005; Evans et al., 2016, 2018b; Evans, 2018). Macrofabric is based on the dip and azimuth (orientation) of the A-axes of clasts predominantly in the range of 30–125 mm (A-axis length), based on the principle that clast A axes will tend to rotate to parallelism with the direction of shear in a Coulomb plastic medium like till (c.f., March, 1932; Ildefonse and Mancktelow, 1993; Hooyer and Iverson, 2000). Fabric data were plotted on spherical Gaussian weighted, contoured lower hemisphere stereographic projections, using Rockware™ software. Statistical analysis was undertaken using eigenvalues (S_1, S_2, S_3), based on the degree of clustering around three orthogonal vectors (V_1, V_2, V_3), presented in fabric shape ternary diagrams (Benn, 1994). This identifies end-members as being predominantly isotropic fabrics ($S_1S_2 \sim S_3$), girdle fabrics ($S_1S_2 \gg S_3$) or cluster fabrics ($S_1S_2 \sim S_3$) and allows visual categorization of samples according to their isotropy and elongation.

Clast form was analysed from diamictons and matrix-supported gravels using 30 or 50 clasts depending on unit thickness. This involved assessments of Powers roundness and clast shape following procedures outlined by Evans and Benn (2004) and Lukas et al. (2013), whereby RA, average roundness and C40 values were derived and plotted on co-variance graphs to facilitate comparisons with deposits of known origin.

The samples for microstructural analysis were collected using 10 cm square, aluminium Kubierna tins, which were cut into the face of each exposure in order to limit sample disturbance. The location, orientation, depth and way-up of the sample were marked on the outside of the tin during collection. Orientated samples are collected so that kinematic indicators (Passchier and Trouw, 1996; van der Wateren et al., 2000; Phillips et al., 2007),

such as the sense of asymmetry of folds and fabrics, as well as the sense of displacement on faults, could be established and used to provide information on the former stress regime. It is important that the orientation of the samples relative to the presumed direction of ice-push is established, as only thin sections cut parallel to this principal stress direction will exhibit the most complete record of deformation and its intensity. A total of 8 orientated samples were collected from within the detachments identified within the glactectonised part of the sequence for detailed micromorphological and microstructural analysis. Two samples (HAY 1 and 2) were taken from a prominent detachment (thrust) affecting the well-bedded sands and gravels towards the top of the sequence. A further six samples (HAY 3 to 8) were collected from a subhorizontal thrust with associated asymmetrical folding developed within the rhythmically laminated sands, silts and clays.

Sample preparation (c. 10 months) involved the initial replacement of pore-water by acetone, which was then progressively replaced by a resin and allowed to cure. Large format orientated thin sections were taken from the centre of each of the prepared samples, thus avoiding artefacts associated with sample collection. Each thin section was cut orthogonal to the main deformation structures evident from the field investigation. The thin sections were examined using a standard Zeiss petrological microscope. Successive generations of both macro- and microscale fabrics, folds (e.g., F1 or earliest to Fn last) and faults are distinguished by the nomenclature normally used in structural geological studies (c.f., Phillips and Auton, 2000; Phillips et al., 2007, 2011a,b). The interrelationships between these structures were also established, enabling the investigation of the deformation history recorded by these deposits and the processes operating during the propagation of the thrust faults.

3. Regional setting & location of study area

The Quaternary deposits of the valley floor and lower slopes of upper Teesdale between Barnard Castle and Middleton-in-Teesdale were emplaced by a glacier which occupied Teesdale at the junction of the Stainmore Gap. This is where Northern Pennine (Teesdale) ice and the regional Stainmore Ice Stream were coalescent but gradually decoupled at the close of the last (Devensian) glaciation (Evans et al., 2018a,b). This decoupling is recorded by an inset series of broad arcuate moraines that demarcate the ice margins at four distinct stages (Fig. 2), including the Glacial Lake Egglehope, Mill Hill, Gueswick and Hayberries stages, as the Teesdale glacier became progressively confined within the Teesdale valley (Evans et al., 2018a,b). In the area between Mickleton and Romalldkirk, immediately east of Middleton-in-Teesdale, the Quaternary deposits form gently undulating to locally hummocky terraces (between 220–230 m OD) composed of glacial outwash deposits (Mills and Hull, 1976; Fig. 3). These include boulder to cobble gravels indicative of high-discharge sedimentation, with clast imbrication recording an easterly palaeoflow (Evans et al., 2018a,b). The undulatory surface of these deposits is thought to reflect the burial and subsequent decay of residual glacier ice as sub-marginal streams produced first glacier karst and then proglacial fans in response to tunnel enlargement and sediment infilling. The eastern-end of the Mickleton-Romalldkirk glacial assemblage includes a series of distinct sinuous ridges composed of sand and gravel and referred to as the Romalldkirk esker complex by Evans et al. (2018a,b).

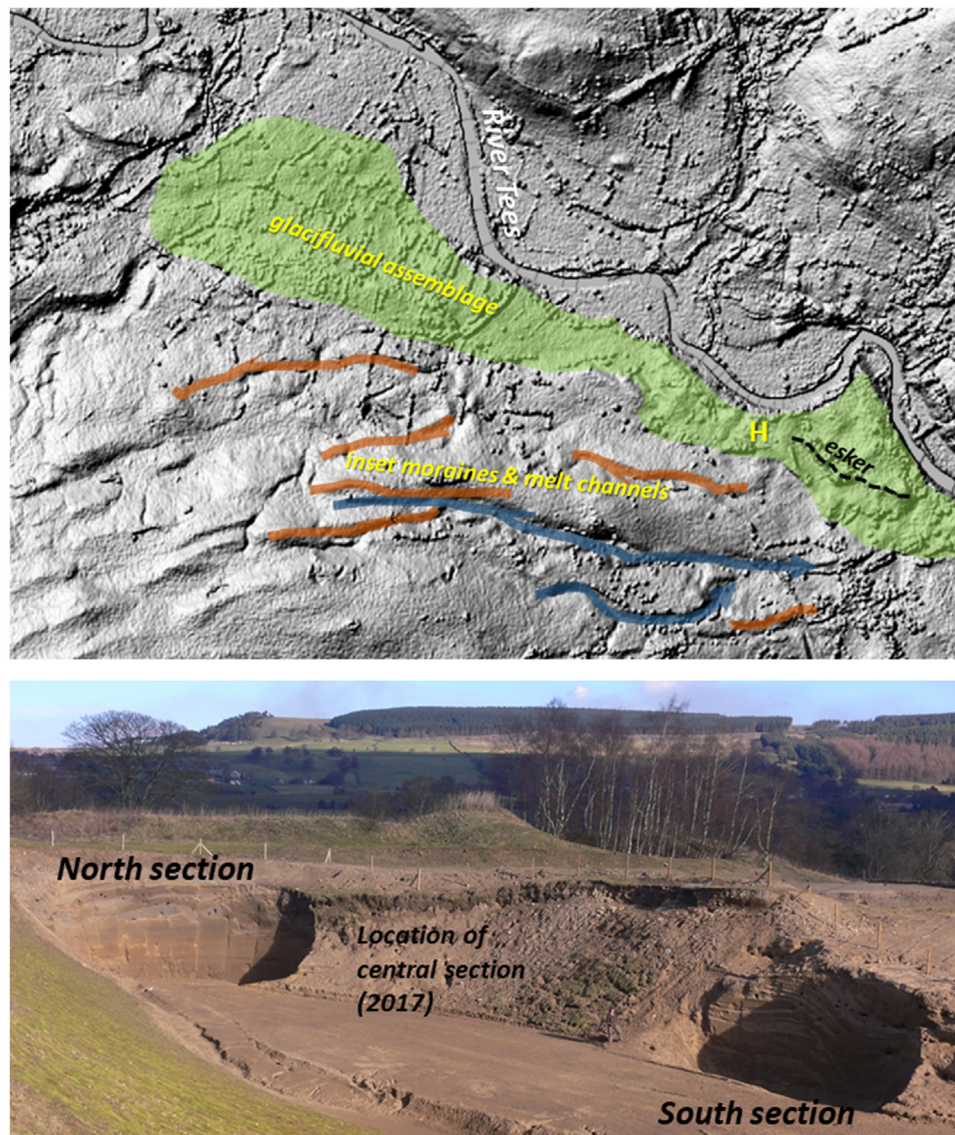


Fig. 3. Annotated NEXTMap digital elevation model (upper) and ground photograph of the Hayberries quarry (lower) showing the positions of the three main section faces. Major lateral moraines (brown lines) and meltwater channels (blue arrows) on the DEM show the pattern of ice marginal recession into Teesdale. Inset within the lowest of the moraines is the Mickleton–Romaldkirk glacifluvial assemblage (green), within which the Hayberries Quarry (H) and the main Romaldkirk esker ridge (black broken line) are marked. (For interpretation of the references to colour in this figure legend, the reader is referred to the web version of this article).

This study focuses upon the glacial sequence exposed at Hayberries quarry [NZ 991 229] located at the western-end of the Romaldkirk esker complex (Fig. 3). At this locality the glacial sediments comprise a sequence of rhythmically bedded sands, silts and clays that coarsen upwards into glacifluvial sands and gravels, deformed in their upper layers. This sequence is scoured and filled by further, undeformed, glacifluvial sand and gravel facies containing and capped by two, generally thin, tills which relate to the emplacement of the esker ridge at Hayberries.

4. Glacigenic sediments and macroscale deformation structures

The sedimentary sequence at Hayberries comprises three main lithofacies associations (LFAs 1–3; Fig. 4). A relatively thick sequence of fine-grained sand, silt and clay rhythmics comprise LFA 1, which is indicative of deposition within a proximal glacial setting, likely one dominated by distal foreset sedimentation (Evans et al., 2018a,b). This grades vertically into LFA 2, comprising sand and gravel deposited in a high-energy

glacifluvial environment. The sands and gravels of LFA 2, and to a lesser extent the underlying glacial lacustrine sediments of LFA 1, are deformed, with the relative intensity of this deformation increasing upwards through the sequence. This variably glacially deformed sequence is capped by LFA 3, which comprises glacifluvial sands and gravels interbedded with two diamictons. The diamictons are hard, compact deposits which locally possess a subhorizontal fissility and contain striated and/or faceted clasts which define a consistent southerly macrofabric; i.e. features characteristic of subglacial tills. Consequently this sequence is thought to record a switch in the style of sedimentation from till emplacement to meltwater deposition. This sequence is exposed in two sections revealed in 2007 (north and south sections, Figs. 3 and 4a) as a result of cliff maintenance within the quarry, and a central section uncovered in 2017 (Fig. 4b).

The northern section at Hayberries quarry reveals a 5 m thick coarsening-upwards sequence of cyclically or rhythmically bedded glacial lacustrine sands, silts and clays (Fig. 4a) with the upper most beds containing dropstones. These sediments comprise LFA 1 and

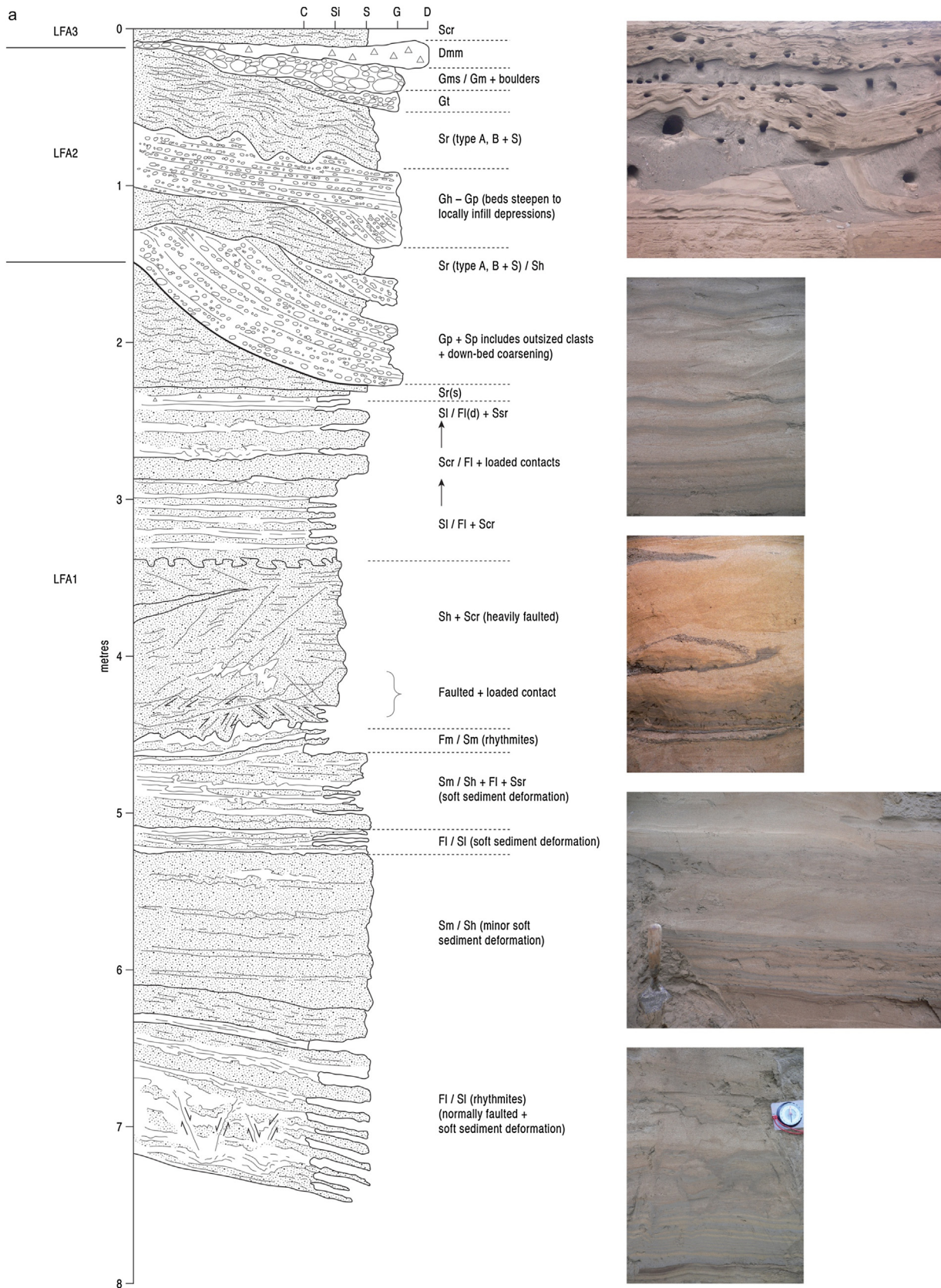


Fig. 4. Stratigraphic and sedimentological details of the northern and central exposures at Hayberries: **(a)** vertical profile log with inset photographs of typical lithofacies types from the north section; **(b)** annotated photomosaic of the northern and central sections, showing stratigraphic architecture, lithofacies types and clast macrofabric and shape data; and **(c)** covariance plot of RA% versus C40% based on clast form data.

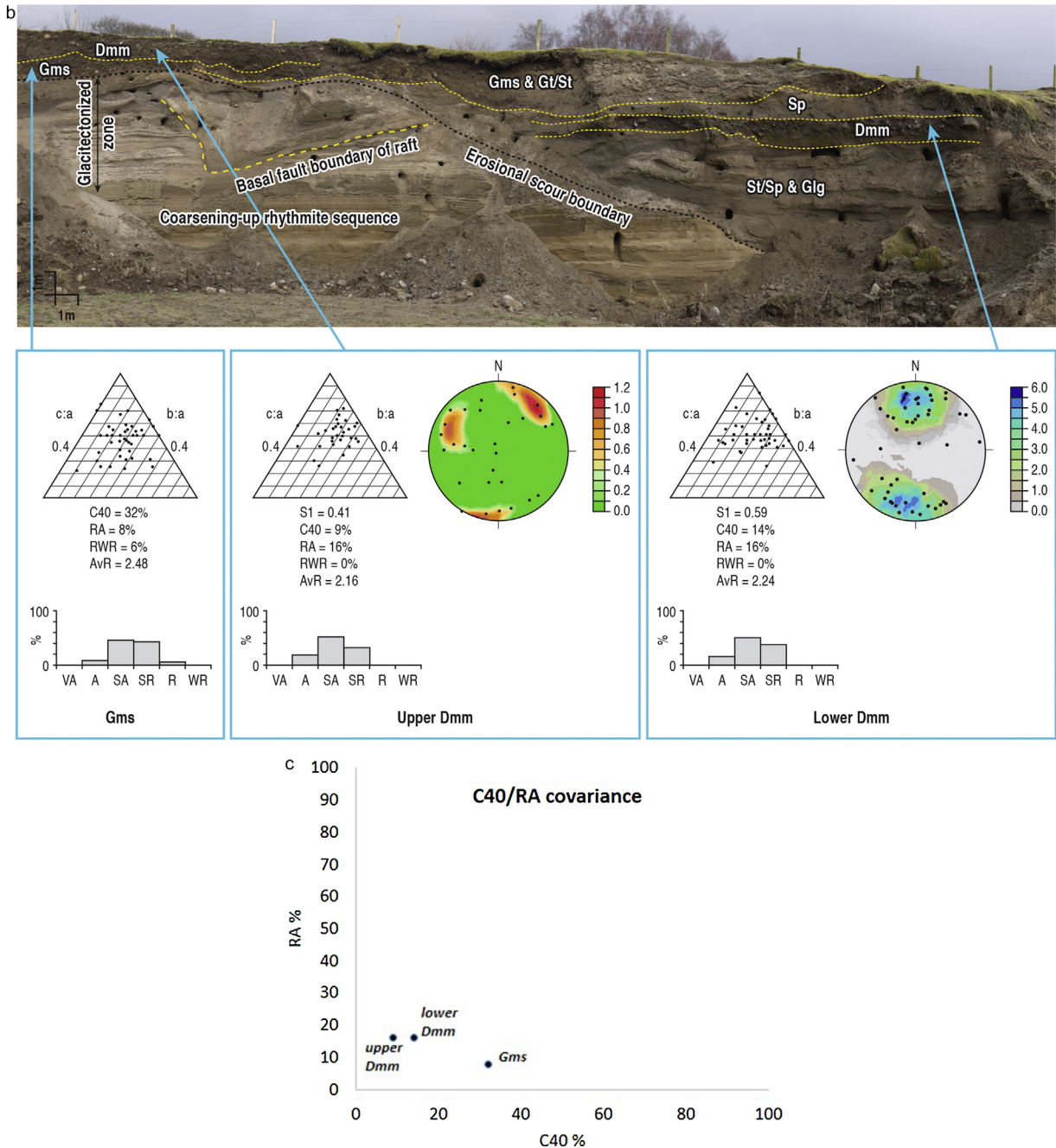


Fig. 4. (Continued)

display characteristics of deepwater sedimentation punctuated by phases of traction current activity recorded by the presence of beds of relatively coarser, ripple drift, climbing ripple and cross-bedded sand. Cyclical changes in grain size from silt/clay to sand may potentially represent seasonal rhythmites or varves (Fig. 4a). Soft-sediment deformation structures occur throughout the lower part of the sequence, including normal faults which offset bedding to form small extensional grabens. Normal faulting is also common within the middle part of the sequence where the sands have been subject to tensional failure.

The glacialacustrine deposits of LFA 1 also occur in the southern section (Fig. 6) where the well-bedded sandy upper part of this sequence is deformed by an open, steeply inclined, asymmetrical anticline-syncline fold pair which occurs within the hanging-wall

of a moderately inclined, south-dipping normal fault (Figs. 6 and 7). Structurally lower in the sequence, this fault is defined by a single prominent planar dislocation with a downthrow to the south. However, higher in the section, towards its tip, the fault is marked by a 20–30 cm wide zone of deformation comprising several irregular to curved fracture planes (Fig. 7). Folding within the hanging-wall of the fault shows a clear spatial relationship with this extensional brittle structure. The open, asymmetrical, south-verging anticline occurs directly above the fault tip, giving the appearance that the well-bedded sands have been “draped” over the fault. The associated syncline is developed within the hanging-wall of the fault, with the beds of pale-coloured sand clearly being locally truncated, or thinning onto the southern limb of the fold (Figs. 6 and 7). In contrast, the more resistant silt or silty

sand layers remain a constant thickness around the fold. Deformation within the footwall of the extensional fault is restricted to a number of small-scale normal faults (displacements < 20–30 cm) and localised drag-folding of bedding immediately adjacent to the main fault system (Figs. 6 and 7). The sense of offset (downthrow to the south in this plane of section) and orientation of the small-scale faults suggests that they are related to the larger scale normal fault (i.e. formed in response to the same extensional deformation).

In the northern section the glacialustrine sediments are conformably overlain by LFA 2, comprising coarser-grained glacialuvial sands and gravels (c. 2.0–2.5 m thick) characterised by the presence of inter-stratified units of planar to horizontally and locally trough cross-bedded, fine- to medium-grained, dark grey coloured gravel (Figs. 4a and 5). On the western side of this section the gravels are interstratified, with the coarser sands occurring at the top of the underlying rhythmite sequence, both units having been folded and thrust (Fig. 8). This relationship records a vertical continuum from glacialustrine rhythmites into the overlying glacialuvial sands and gravels, consistent with the progressive shallowing of water depths prior to deformation. Elsewhere the base of the gravels cut (erode) downward into the underlying sandy upper part of the glacialustrine sequence (Figs. 8 and 9a). Bedding within the gravels appears to steepen to form concave erosional (scoured) contacts with underlying sands, with the gravels locally forming clinofolds or foresets typical of transverse fluvial bars. Both bedding and the erosional bases to the gravels have been variably modified by deformation to form low-angle to moderately (15° – 30°) N- to NW-dipping (Fig. 5), and NE-directed (in this plane of section) thrusts (Figs. 8–11). The maximum amount of displacement on these thrusts is in the order of a few meters, with thrusting resulting in the localised repetition and stacking of the gravels (Figs. 10 and 11a). Although the thrusts appear to be sharp, planar structures, in detail they are marked by a thin zone (≤ 10 – 15 cm) of massive to foliated sand or fine-gravel. The thinly bedded sands and gravels within the hanging-walls of the thrusts are deformed by open, asymmetrical east- to southeast-verging anticlines and synclines (Figs. 8, 9b and 10). Small-scale minor folds (amplitudes 20–30 cm), which possess Z, S and M geometries, are parasitic upon these mesoscale

structures (Figs. 8 and 9b). The geometry of the folds and sense of displacement on the thrusts are consistent with an applied stress from the north or northwest. Locally the folds are observed to have deformed earlier developed thrusts, indicative of several phases of thrusting (Fig. 10).

Importantly this deformed sequence is unconformably capped by a laterally extensive matrix-supported gravel (Gms) which in turn overlain by a compact and locally weakly fissile but otherwise macroscopically massive (i.e. in the field), matrix-supported diamicton (Dmm). The contact between the Gms and Dmm is sharp but intermixed, with the base of the diamicton being characterised by the presence of a relatively higher concentration of clasts derived from the underlying gravels. Clast sizes then increase vertically (inverse grading) in the diamicton. Clast forms in the Gms (Fig. 4b) are sub-angular to sub-rounded (RA = 8%; RWR 6%; average roundness = 2.48) with a C40 value of 32%, typical of glacialuvial outwash (c.f., Lukas et al., 2013). In contrast, clast forms in the Dmm (Fig. 4b) are markedly more blocky (C40 = 9%) and more sub-angular (RA = 16%; RWR = 0%; average roundness 2.16) and no clasts display striae, suggesting subglacial reworking of glacialuvial materials. The covariance plot of all clast form samples from Hayberries (Fig. 4c) indicates a predominantly subglacial signature (cf. Benn and Ballantyne, 1994; Lukas et al., 2013). A clast macrofabric from the Dmm (Fig. 4b) is essentially isotropic (S1 = 0.41) but displays a very weak northerly girdle. The characteristics of the Dmm suggest that it is a subglacial traction till (*sensu* Evans et al., 2006; Evans, 2018) derived directly from the underlying glacialuvial deposits, from which it is separated by an amalgamation or shear zone (Fig. 6); deformation appears to have been imparted by glacier stress from the north but the clast macrofabric signature of this is not strong likely because of the high clast content and resulting clast interference effects (c.f., Evans et al., 2016; Evans, 2018). Lithic clasts (including striated and faceted clasts) within the till are predominantly of locally derived Carboniferous sedimentary and Whin Sill provenance, with no unequivocal erratic material and hence the till has been emplaced by the Teesdale-sourced ice.

The recently exposed central section at Hayberries quarry reveals that the glacial tectonised sequence has been incised/scoured to a maximum depth of c. 3 m. The resulting channel-like feature is

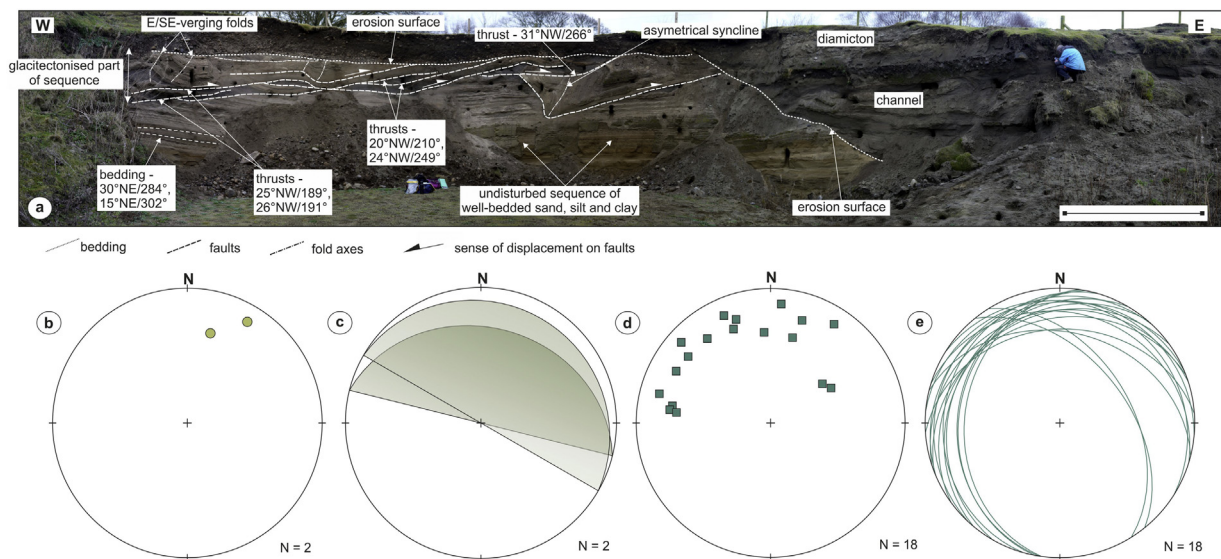


Fig. 5. (a) Interpreted photomosaic showing the stratigraphic, sedimentological and structural details of the northern section at Hayberries Quarry (scale bar = 3 m); (b) and (c) Lower hemisphere stereographic projections showing the dip and dip direction (b) and dip and strike of bedding planes (c) within the glacialustrine sequence; (d) and (e) Lower hemisphere stereographic projections showing the dip and dip-direction (azimuth) of the thrusts (d) and dip and strike of the thrust planes (e).

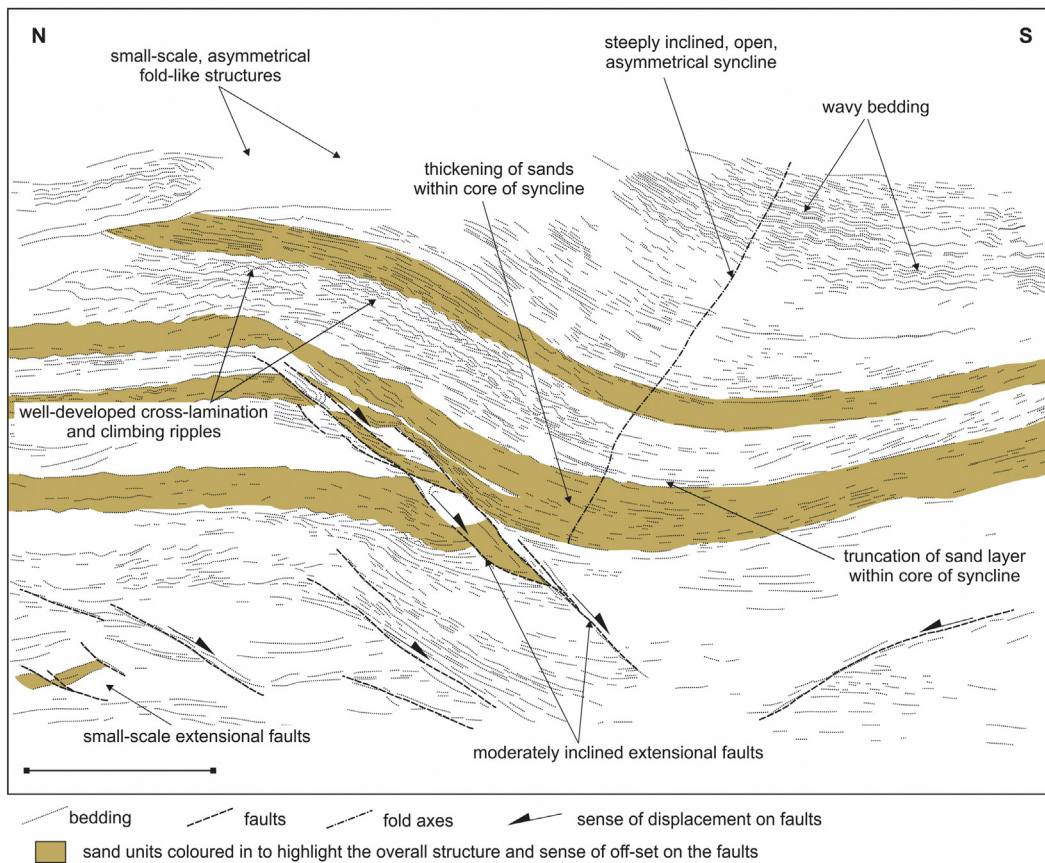
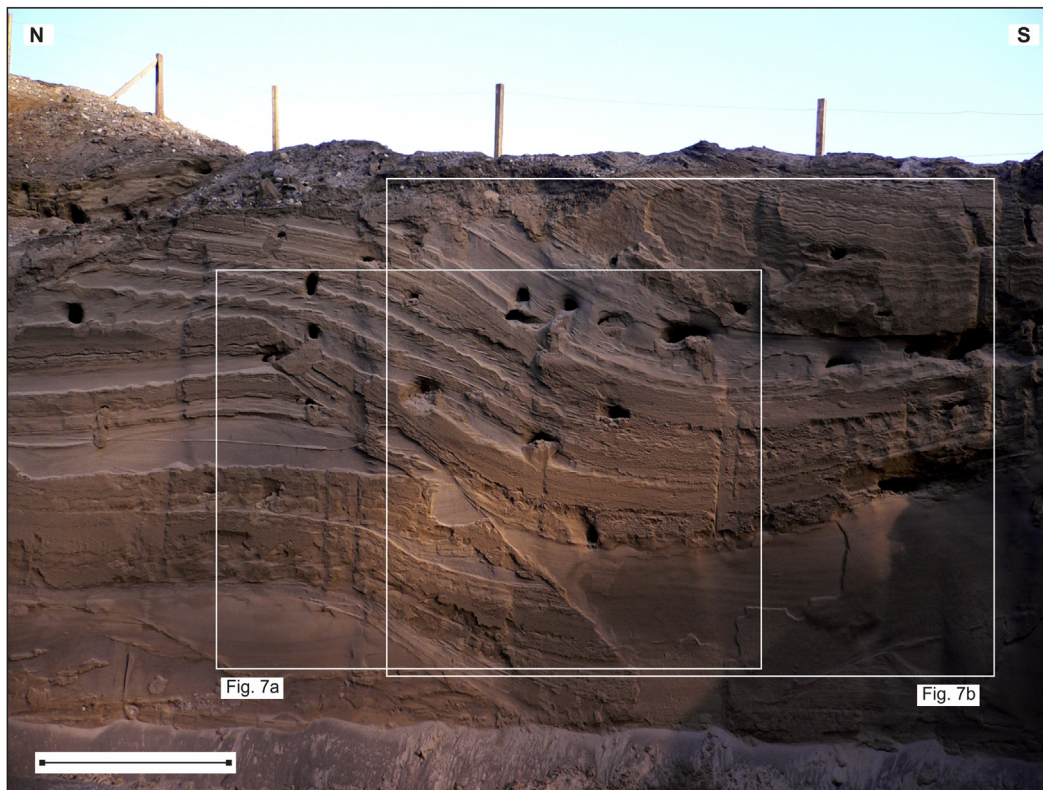


Fig. 6. Structural interpretation of the southern section at Hayberries Quarry showing the relationship between a large scale anticline-syncline fold pair and a structurally underlying normal (extensional) fault. Also shown are the location of the photographs illustrated in Fig. 7 (scale bar = 2 m).

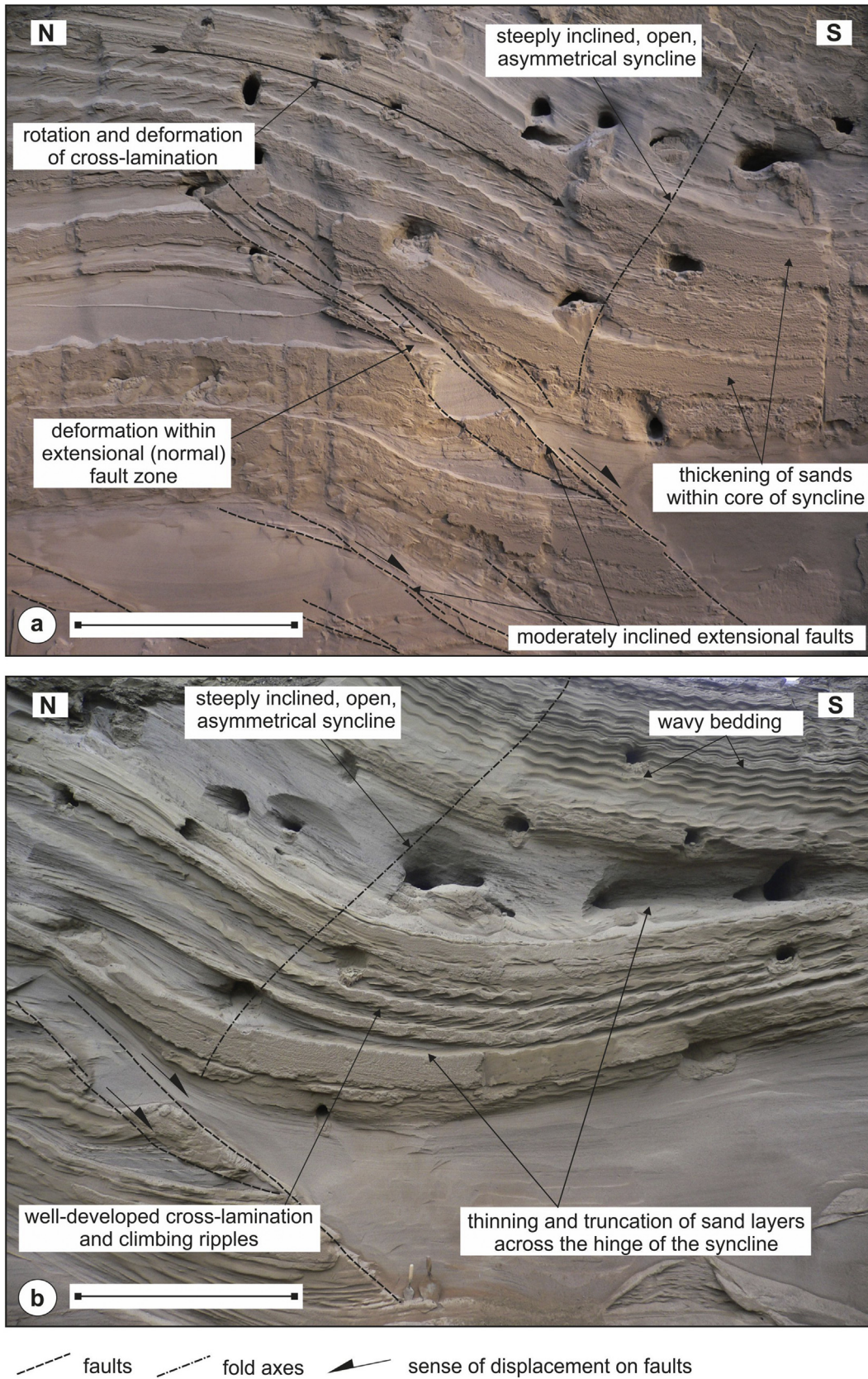


Fig. 7. (a) Southerly verging anticline and syncline fold pair developed above a southerly dipping normal (extensional) fault (scale bar = 1.5 m); and (b) Thinning and truncation of sand and silty sand layers across the syncline developed within the hanging-wall of a syndepositional normal fault. Note the well-developed cross-lamination and climbing ripples within the silty sands (scale bar = 1 m).

infilled with a horizontally stratified sequence of cross-bedded coarse sands and gravel lags, and minor gravel beds (Figs. 4b and 5). Importantly these sediments show no obvious evidence of deformation (Fig. 5), indicating that the phase of incision and sedimentation post-dated glacetectonism. These channel-fill deposits are themselves truncated by a thin (c. 30 cm) macroscopically massive, matrix-supported diamicton (Dmm) with diagnostic subglacial clast forms (RA = 16%; C40 = 14%; RWR = 0%; average roundness 2.24) and a moderately strong clast macrofabric (S1 = 0.59) aligned N–S and dipping preferentially northwards (Fig. 4b). This Dmm is interpreted as a subglacial traction till (*sensu* Evans et al., 2006; Evans, 2018), which records ice advance from the north. Lithic clasts within the diamicton are of predominantly locally derived Carboniferous sedimentary and Whin Sill provenance with only a small percentage (4% wacke sandstone) being of a more far travelled (erratic) provenance. The till is in turn overlain by a coarsening-upward sequence of coarse-grained, planar-bedded sands passing upwards into interstratified units of matrix-supported and locally clast-supported, cobble to pebble gravel and trough cross-bedded sand and gravel typical of ice-

proximal glaci-fluvial sediments (c.f., Miall, 1977, 1978). Importantly, these coarse and poorly-sorted gravels are continuous with those that cap the northern section, thereby indicating that two diamictons (tills) are interbedded with ice-proximal glaci-fluvial outwash deposits and are hence classified as LFA 3. In summary based upon the northern and central sections (Fig. 4), LFA 3 comprises, in vertical sequence, coarsening up glaci-fluvial sands and gravels (St/Sp and Glg), lower till (Dmm), proximal glaci-fluvial gravels and sands (Gms and Gt/St) and upper till (Dmm) indicative of a switching depositional regime in which an environment of high meltwater discharge alternated with subglacial till emplacement. The northerly dipping clast macrofabrics from the two tills are related to ice flow towards the southern slopes of this part of the Teesdale valley, which is compatible with the flow vectors in a lobate glacier snout occupying the valley floor at this location during the Gueswick and Hayberries stages (Evans et al., 2018a,b; Fig. 2b).

Based upon the sedimentological descriptions and interpretations outlined above, Evans et al. (2018a,b) have proposed that the Hayberries stratigraphy records a sequence of depositional

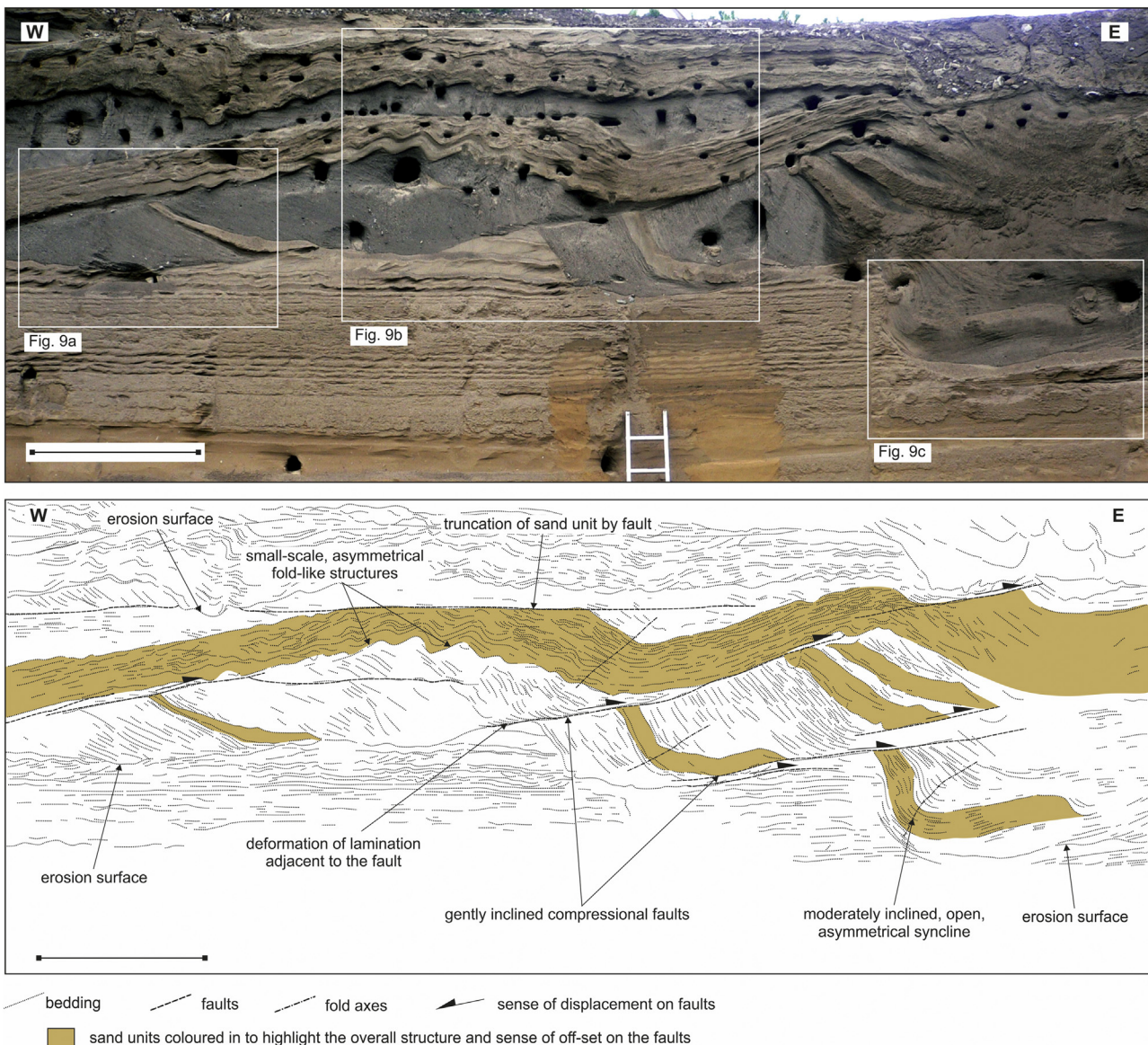


Fig. 8. Structural interpretation of part of the northern section at Hayberries Quarry showing the relationships between E-SE-directed thrusts and large scale asymmetrical folds. Also shown are the location of the photographs illustrated in Fig. 9 (scale bar = 2 m).

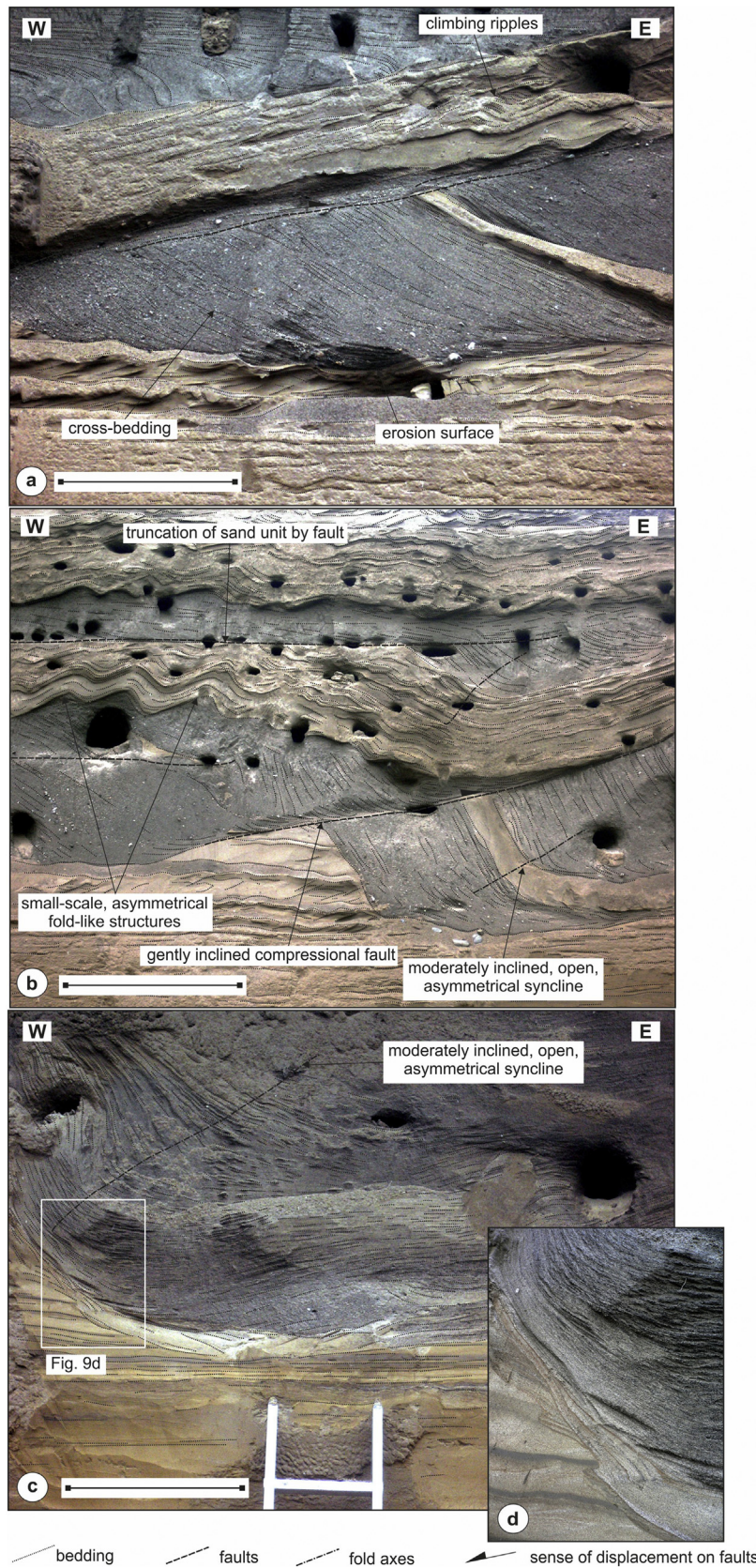


Fig. 9. (a) Close up of variably deformed glacial sands and gravels overlying relatively sand-rich glacial sequence, showing steepened (rotated) crossbedding within the dark coloured gravels due to deformation (scale bar = 1 m); (b) E/SE-verging asymmetrical folds and E/SE-directed thrusts deforming the glacial sands and gravels (scale bar = 2 m); and (c) Tectonised sedimentary contact between the gravel and underlying thinly bedded sand, silt and clay (scale bar = 1 m).

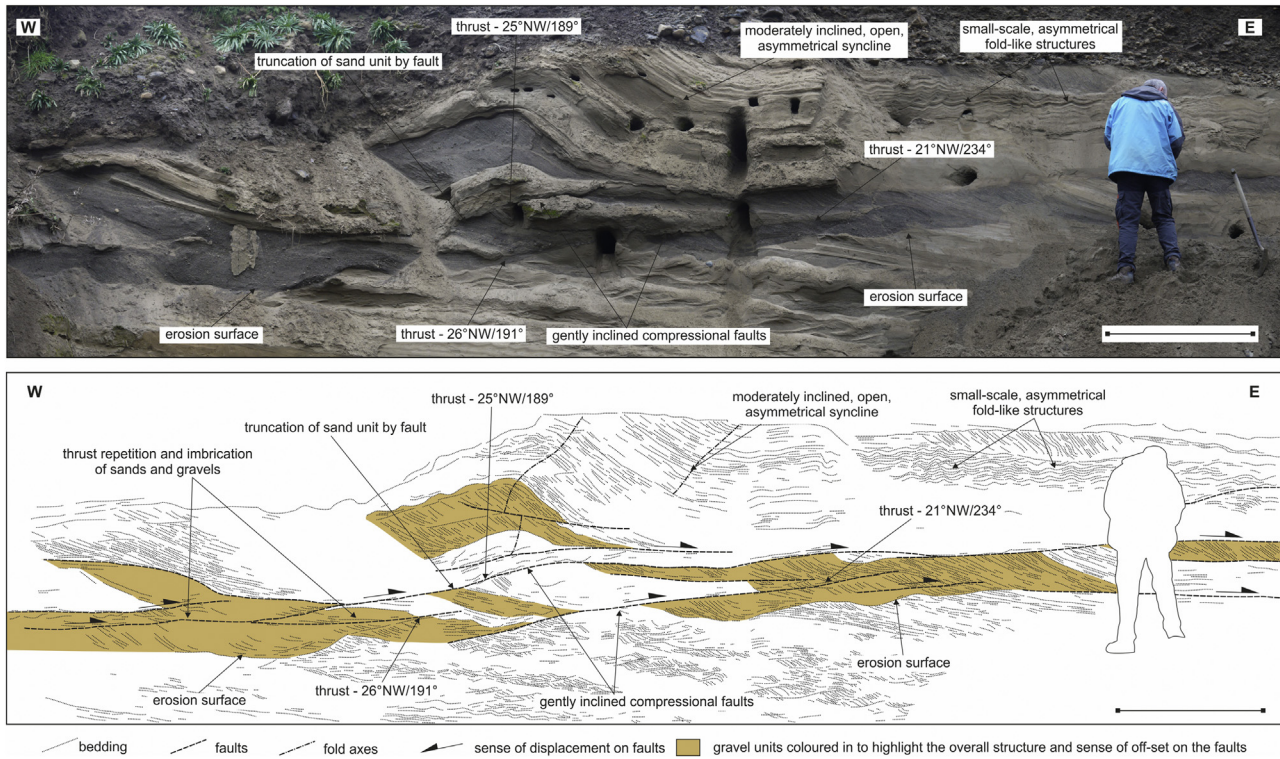


Fig. 10. Structural interpretation of part of the northern section at Hayberries Quarry highlighting the localised (minor) imbrication of the glaci-fluvial sands and gravels associated with low-angle E/SE-directed thrusting (scale bar = 1.5 m).

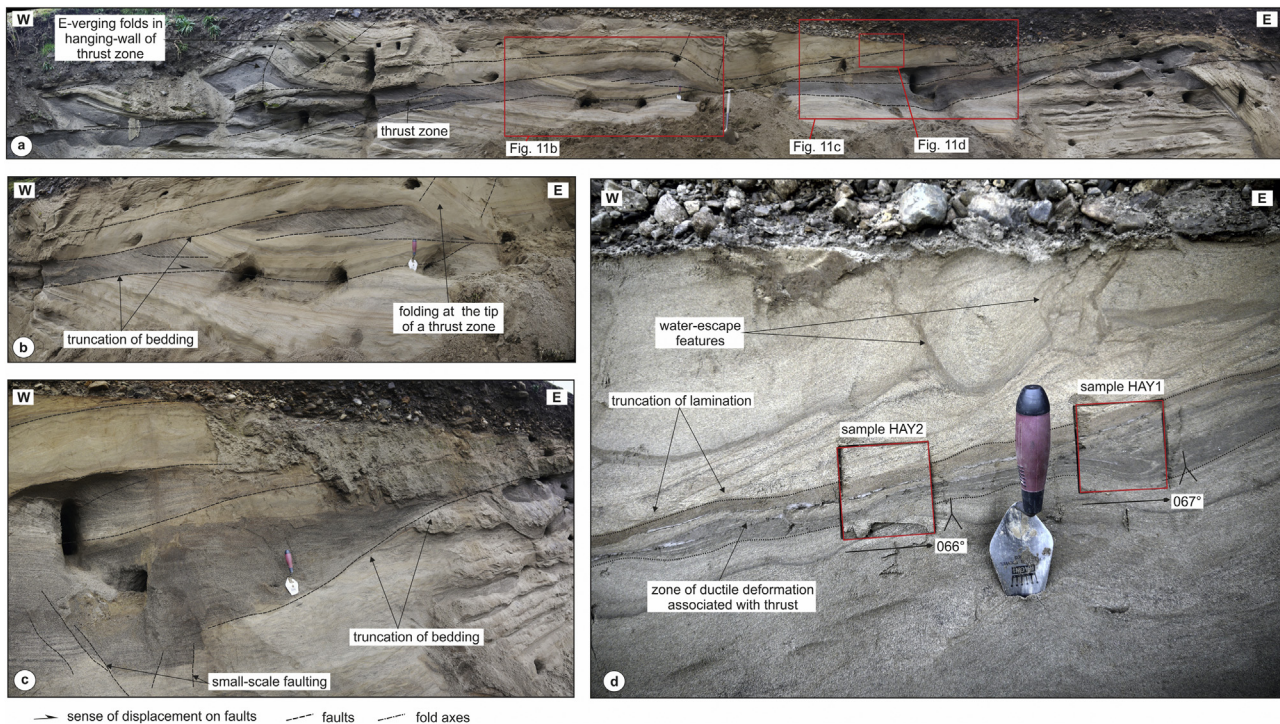


Fig. 11. (a) Structural interpretation of the northern section Hayberries Quarry highlighting the localised (minor) imbrication of the glaci-fluvial sands and gravels which dominate the upper part of the sequence; (b) Truncation of early formed folds and bedding within the glaci-fluvial sands and gravels due to low-angle thrusting; (c) Thrusting within the glaci-fluvial sands and gravels truncated at the base of the overlying diamict; and (d) Location of samples HAY 1 and 2 collected from a 5–10 cm wide zone of apparently ductile deformation marking one of the NW-dipping thrusts.

environments that relate to the sequential development of lobate ice margins during deglaciation of upper Teesdale (Fig. 2). The existence of an infilling proglacial lake in the area is clearly

evidenced by the rhythmites of LFA 1 and coarsening-upwards sequence of sands and gravels of LFA 2. These sediments were then glaci-tectonically deformed implying that a glacial readvance into a

proglacial moraine-dammed lake (the Hayberries Stage; see discussion) occurred after ice retreated from the Gueswick Hills moraine assemblage (Fig. 2b). We now focus on the remarkable glacitectonic structures created during the Hayberries Stage.

5. Microscale deformation structures

Eight thin sections were collected from the thrust zones within the glacitected glaciﬂuvial and glacialustrine sequences (Figs. 12–20) in order to examine the microscale deformation structures developed within these detachments and investigate the processes occurring during the initial propagation and subsequent evolution of these structures.

5.1. Deformation structures associated with thrusting of the glaciﬂuvial sequence

One of the detachments deforming the glaciﬂuvial sands and gravels of the upper part of the sequence in the northern section at Hayberries (Fig. 11a, d) was selected for more detailed microstructural analysis. This gently NW-dipping thrust is marked by a c. 10 cm thick zone of finely stratified sand, silt and minor clay (Fig. 11d). The stratification occurs coplanar to the bounding surfaces of the thrust zone and is locally deformed by asymmetrical, gently inclined, tight to isoclinal folds (see Fig. 11d) and small-scale, low-angle faults and shears with apparent displacements of a few millimetres to centimetres. The upper boundary of this zone of predominantly ductile deformation clearly truncates a fine-scale lamination or cross-lamination within the pale coloured sands in the hanging-wall of the thrust (Fig. 11d). Bedding within the hanging wall is further disrupted by a network of water-escape features filled by apparently massive, darker coloured fine-grained sand. The thrust is clearly truncated at the base of the overlying diamicton (Fig. 11a, c) and therefore predates the accretion of this subglacial traction till.

Two thin sections were taken from the thrust zone (HAY 1 and 2; Figs. 11d, 13 and 14). In thin section HAY 1 (Fig. 13) the sands within the hanging-wall of the thrust occur at the top of the thin section. The zone of deformation marking the thrust can be divided into three subzones: (i) a 15–20 mm thick area at the top of the thrust zone composed of two weakly laminated to massive sand layers separated by a 2–4 mm thick layer of normal graded (fining upwards) silt and clay (Fig. 13). The sand possesses a distinctive red-brown clay matrix partially infilling the pore spaces and is apparently undeformed. The lamination, where developed, is apparently coplanar to the upper bounding surface of the thrust zone; (ii) a wedge-shaped unit of massive to finely laminated, fine-grained, matrix-poor sand and silty sand which is folded by a number of tight to isoclinal, recumbent microfolds developed within the hinge zone of a larger “synform”. The hinge zone of this

fold is further deformed by a number of closely spaced subhorizontal NE-directed (in this plane of section) thrusts and gently NE-dipping, low-angle normal faults (Fig. 13). These brittle faults clearly offset the limbs of the recumbent microfolds and possibly developed in response to the tightening of the larger synform; and (iii) a lower subzone composed of finely laminated sand, silty sand and silt deformed by an isoclinal recumbent “antiform”. The nose of this fold appears “pinched” (see Fig. 13) suggesting that it has been compressed (tightened) possibly in response to loading occurring in response to the tectonic thickening of the sediment pile. The gently NE-dipping lamination on the upper limb of this fold is clearly truncated by the subhorizontal thrusts which characterise subzone (ii). These subzones can also be identified on a macroscale (see Fig. 11d). The boundary between subzones (i) and (ii) is locally marked by a thin elongate lens of clay (Fig. 11d). This boundary also appears to cross-cut the microfaults present within subzone (ii).

In contrast to sample HAY 1, in thin section HAY 2 the laminated sediments within the thrust zone show no obvious evidence of either brittle (faulting) or ductile (folding) deformation (compare Figs. 13 and 14). The three subzones identified in HAY 1, although they are much thinner, can be traced down-dip within the thrust into HAY 2. Subzone (i) is composed of a weakly laminated to massive sand which possesses a distinctive red-brown clay matrix (Fig. 14). The folding and faulting of subzone (ii) is replaced by a mottled, matrix-poor sand layer occurring between two weakly graded fine silt to clay layers. Although sharp the contacts between the sand and clay layers are highly irregular to flame-like (Fig. 14) and the clays are locally cross-cut by thin sand veinlets. The sand within these veinlets is lithologically similar to the mottled sand which occupies the centre of the subzone. The recumbent folding of subzone (iii) in sample HAY 1 is replaced in HAY 2 by a unit of undeformed weakly laminated to massive, fine- to coarse-sand (Fig. 14). In HAY 2 the stratification within subzone (iii) is clearly truncated against the lower silt-clay layer marking the base of subzone (ii). The laminated, fine- to coarse-grained sand within the hanging and footwalls of the thrust occur at the top and bottom (respectively) of the thin section (Fig. 14).

5.2. Deformation structures associated with thrusting of the glacialustrine sequence

A further six samples (HAY 3 to 8; Figs. 15–20) were collected from two subhorizontal thrusts exposed in the northern section of the quarry, with associated asymmetrical folding, developed within the glacialustrine (LFA 1) sands, silts and clays (Fig. 12). In both outcrop (Fig. 12) and thin section (Figs. 15–20), the dark coloured, finely laminated clays, silts and sands within the hanging-wall of the lower thrust are folded and thrust. The relative intensity of this folding and the disruption caused by the

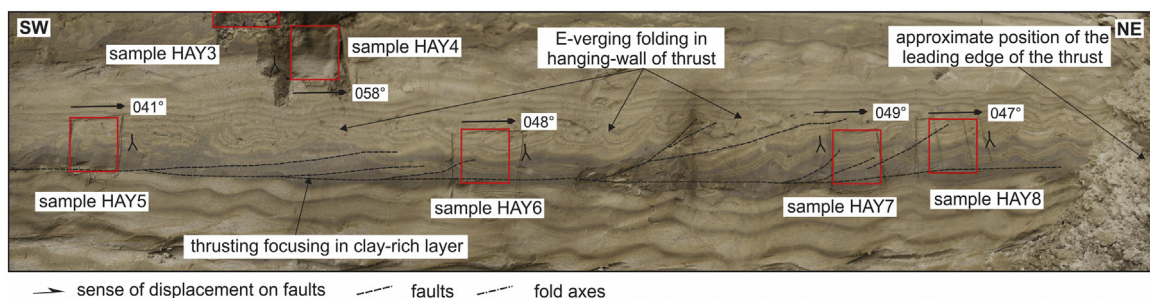


Fig. 12. Photomosaic of a subhorizontal thrust deforming the thinly bedded, glacialustrine sands, silts and clays which dominates the lower part of the northern section at Hayberries Quarry. Note the presence of well-developed asymmetrical folds and minor thrusts in the hanging-wall of the main “basal” thrust. Also shown are the location of the samples HAY 3–8 which were taken for detailed microstructural and micromorphological analysis of the processes during the development of glacitectonic thrusts.

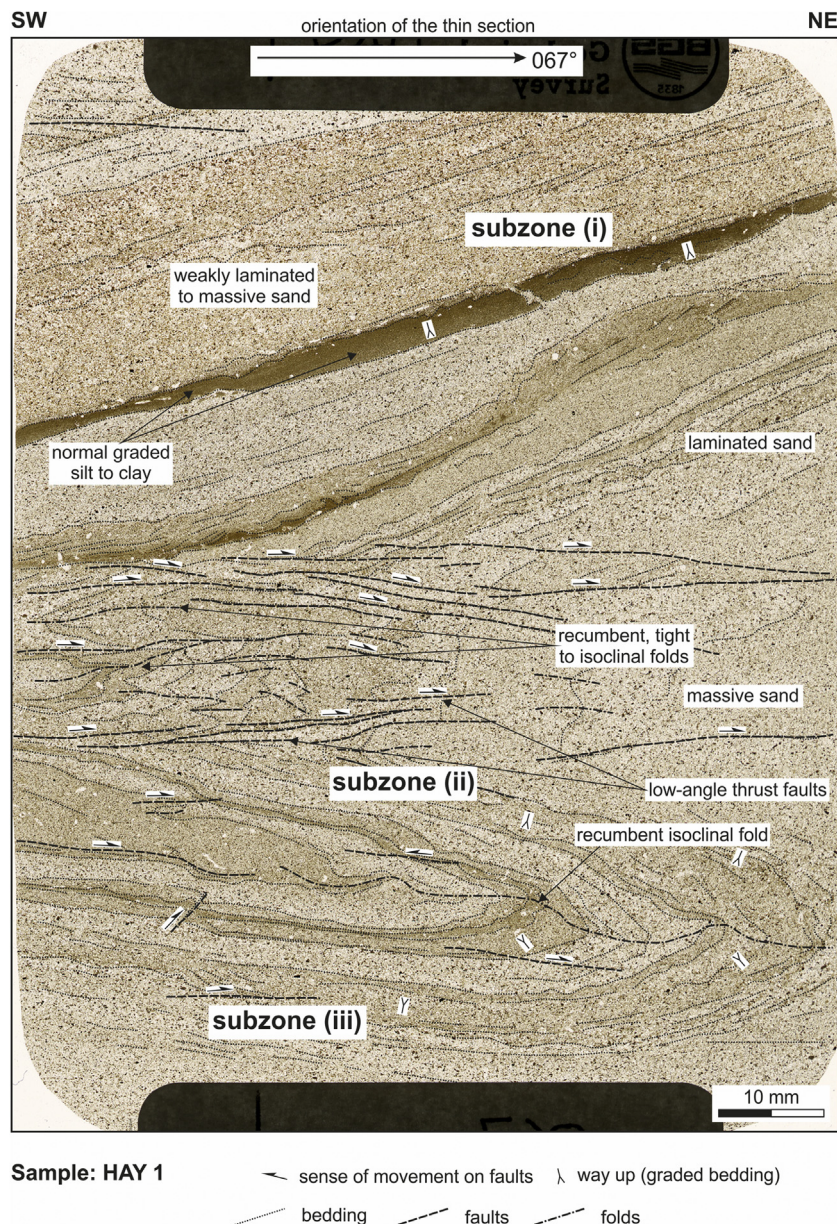


Fig. 13. Annotated high-resolution scan of the large format thin section taken from sample HAY 1 (see text for details). See Figure 11d for details of the location of sample HAY 1.

thrusting increases (in this plane of section) from NE to SW. The thin sections were collected at different points along these thrusts (see Fig. 12) in order to examine the changes in the style of deformation occurring along these structures.

In thin section the individual laminae of sand, silt and clay are graded (normal grading; see Figs. 17–20), indicating that the sequence is in general the right-way-up and only locally overturned on the short, lower limbs of small-scale asymmetrical folds. Variations in the grain size and thickness of these rhythmically laminated sediments reveal the presence of small-scale thinning and fining up-ward cycles (Figs. 18–20); consistent within the overall coarsening upward glacialacustrine sequence identified in outcrop. In contrast the sediments within the footwall of the thrust (e.g. HAY 4, 5, 6 and 7; Figs. 16–19 respectively) are dominated by massive to weakly bedded sand, with the detachment occurring at the boundary between the sands and overlying laminated sequence. This bedding surface would have represented a significant rheological boundary within the deforming pile,

helping to focus thrusting along this lithological contact. This “basal thrust” can be seen in samples HAY 6, 7 and 8, where it separates the folded and faulted rhythmically laminated sediments from the underlying sands (Figs. 18–20).

The thin sections reveal that towards the E/NE-end of the thrust, deformation within the hanging-wall is dominated by asymmetrical E/NE-verging folds (HAY 6, 7 and 8; Figs. 18–20). The steeply inclined to overturned E/NE limbs of these folds are locally cut out by a network of gently W/SW-dipping thrust faults (HAY 7 and 8; Figs. 19 and 20). In sample HAY 7 the thrusting has resulted in the offset and stacking of several folds (Fig. 19). At a structurally higher level within the laminated sequence, bedding is offset by several sets of small-scale E/NE-dipping normal and reverse faults. Further to the W/SW, deformation within the hanging-wall of the thrust is dominated by a number of moderately W/SW-dipping normal faults, which appear to have largely cut-out the hinge zones of the earlier formed E/SE-verging folds (HAY 6; Fig. 18). These extensional faults downthrow to the W/SW.

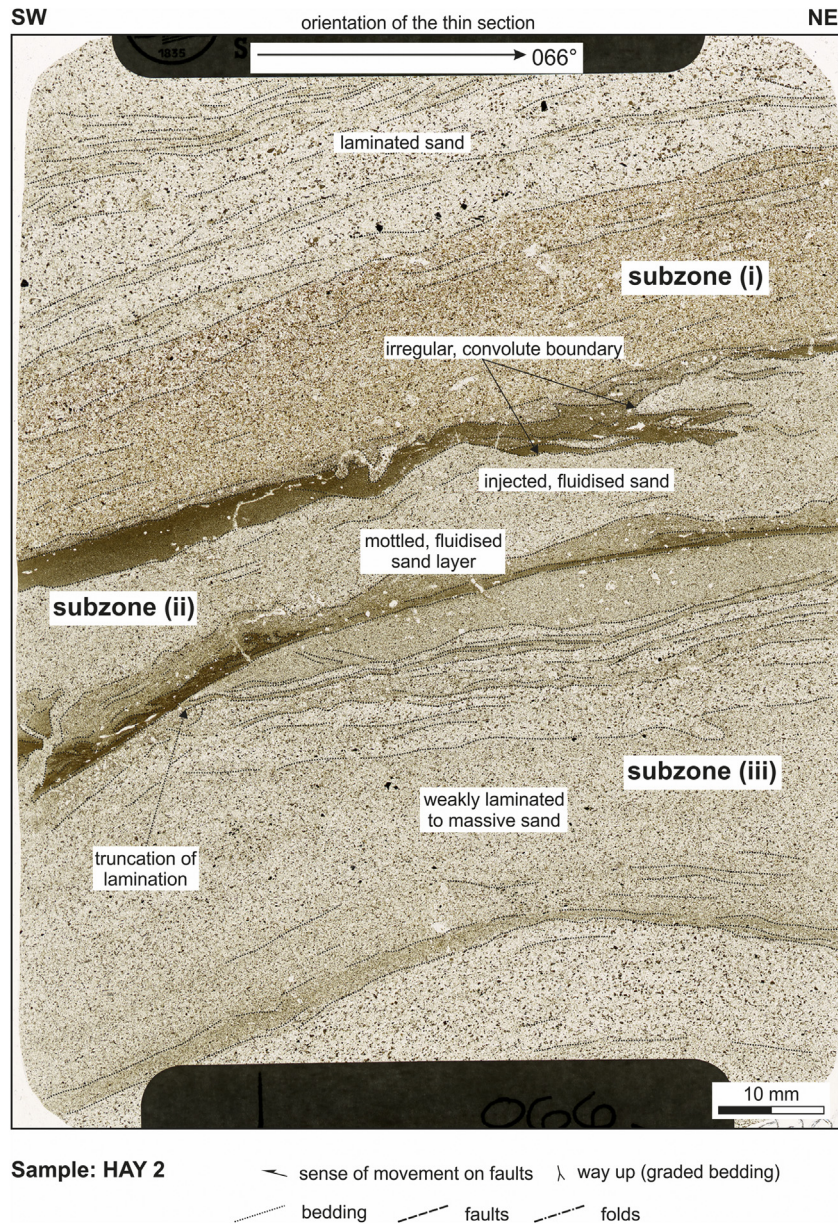


Fig. 14. Annotated high-resolution scan of the large format thin section taken from sample HAY 2 (see text for details). See [Figure 11 d](#) for details of the location of sample HAY 2.

The folded and faulted laminated sediments and “basal thrust” are separated by a 15–25 mm thick massive to very weakly bedded sand which locally thickens within the cores of the anticlines (e.g. HAY 6; [Fig. 18](#)) and is effected by the thrusting which truncates these ductile structures (HAY 7 and 8; [Figs. 19 and 20](#)), as well as the extensional fault zone identified in sample HAY 6 ([Fig. 18](#)). To the W/SW the weak lamination observed in samples HAY 6 and 7 is lost/overprinted, with the sand possessing a distinctive mottled appearance reflected in the modal proportion of a clay matrix (HAY 4 and 5; [Figs. 16 and 17](#)). Furthermore the basal thrust evidence within HAY 6 and 7 ([Figs. 18 and 19](#)) is no longer apparent within samples HAY 4 and 5 ([Figs. 16 and 17](#)) and the sand appears to grade into the underlying laminated sand (e.g. HAY 5; [Fig. 17](#)). The upper boundary of the massive sand clearly cross-cuts bedding within the overlying laminated sediments and can locally be seen forming irregular flame-like features injected along the closely spaced normal faults that deform the sediments in the upper part of the thin section (HAY 5, [Fig. 17](#)). In sample HAY 4 the mottled sand is

connected to a funnel-shaped structure filled by sub-vertically stratified sand and silty sand, with this stratification occurring coplanar to its walls. These characteristics indicate that this is a water-escape feature filled by fluidised sand injected along a pre-existing fault zone ([Fig. 16](#)). The laminated sediments immediately adjacent to the NE-side of the water-escape feature are cut by a number of sub-vertical normal faults, indicating that fluid escape exploited these pre-existing faults. On the SW-side of the water-escape feature, however, the vertically laminated sediments are deformed by complex disharmonic folds.

Sample HAY 3 ([Fig. 15](#)) was collected from a structurally higher position within the glacialacustrine sequence ([Fig. 12](#)) and represents the upper part of a water-escape feature comparable to that seen in HAY 4. In HAY 3 the faulted, rhythmically laminated sediments at the base of the thin section are cut by an apparently fault-guided sand-filled water-escape feature which is connected to an c. 40 mm thick massive sand layer which possesses a distinctive mottled appearance ([Fig. 15](#)). The top of this sand layer

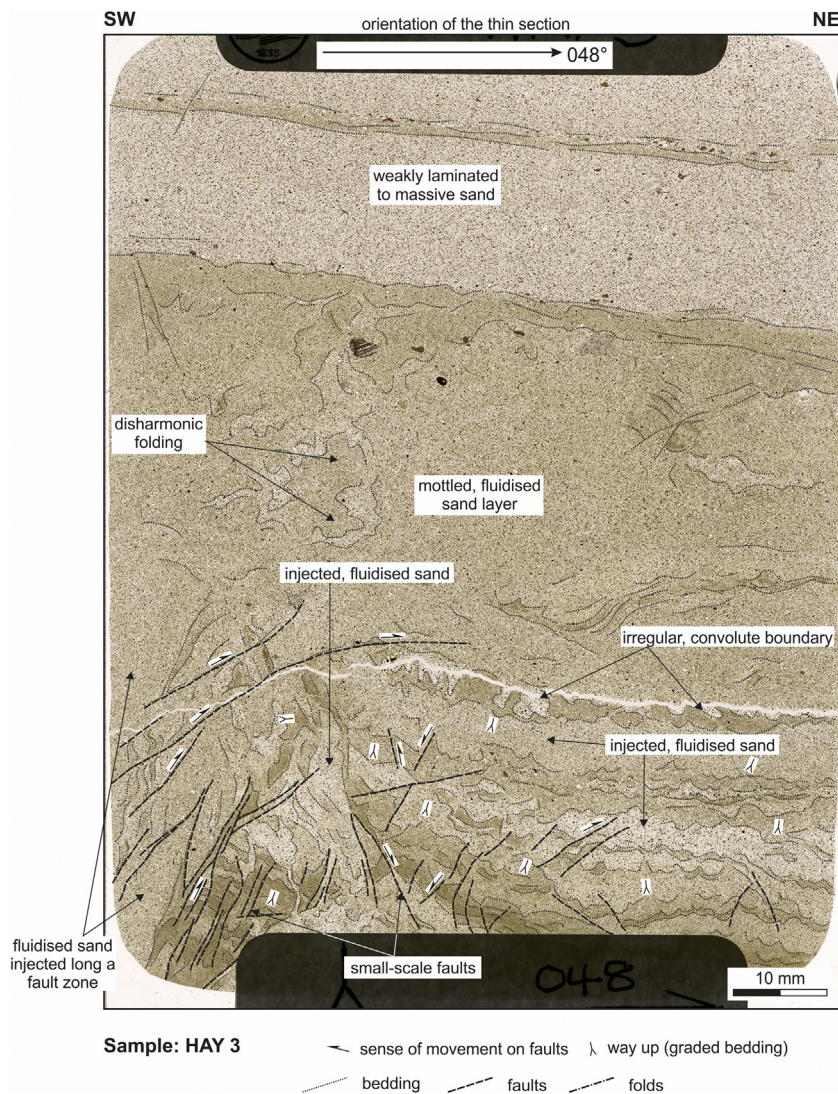


Fig. 15. Annotated high-resolution scan of the large format thin section taken from sample HAY 3 (see text for details). See [Figure 12](#) for details of the location of sample HAY 3.

is sharp. However, its lower boundary with the underlying laminated sediments is highly irregular with a convoluted appearance (see [Fig. 15](#)). A number of irregular sand-filled veinlets were observed both cross-cutting and sub-parallel to bedding within the rhythmically laminated sediments.

6. Interpretation

6.1. Synsedimentary deformation and glactectonism at an oscillating glacier margin

It is clear that the sediments exposed at Hayberries quarry record a sequence of depositional environments commencing with the formation of a proglacial lake, which accommodated the deposition of the rhythmically laminated sands, silts and clays (LFA 1; [Fig. 4](#)). This lake was probably dammed by the Gueswick Hills moraine assemblage ([Fig. 2](#); [Evans et al., 2018a,b](#)). As this moraine reaches an altitude of c. 220 m OD and the top of the Hayberries exposure is below this at < 205 m OD, a moraine-dammed lake is the most likely scenario. As described above, this lake was filled by a thick (c. 5 m) coarsening-upwards sequence of cyclically or rhythmically bedded sands, silts and clays ([Figs. 7 and 8](#)). This apparently deepwater sequence was punctuated by phases of traction current activity leading to the deposition of relatively

coarser cross-bedded to cross-laminated (ripple drift, climbing ripple) sands. The occurrence of dropstones within the upper most part may record the increasing proximity of the ice margin and/or increased bergs calving into the lake.

Soft-sediment deformation structures, in particular normal faults, occur throughout the glacialacustrine sequence. The southerly dipping normal fault and associated asymmetrical anticline-syncline fold pair present within the southern section ([Fig. 6](#)) provides important information regarding the relative timing of this extensional deformation and sedimentation. As described above the south-verging anticline occurs directly above the tip of the normal fault, giving the appearance that the well-bedded sands have been “draped” over this extensional structure ([Fig. 6](#)). The adjacent syncline is located within the hanging-wall of the fault, with the folded beds of sand either thinning onto, or truncated by the southern limb of the syncline ([Fig. 7b](#)). In contrast, the more resistant silts or silty sands retain a constant thickness around this fold. The most likely interpretation of these relationships is that normal faulting and spatially related folding were synsedimentary. Periodic fault movement on the fault would have led to the growth of a shallow depression, occupied by the hinge zone of the developing syncline, as the hanging-wall block progressively lowered. This hollow was subsequently filled by sand which thickens toward the core of the fold. Once the

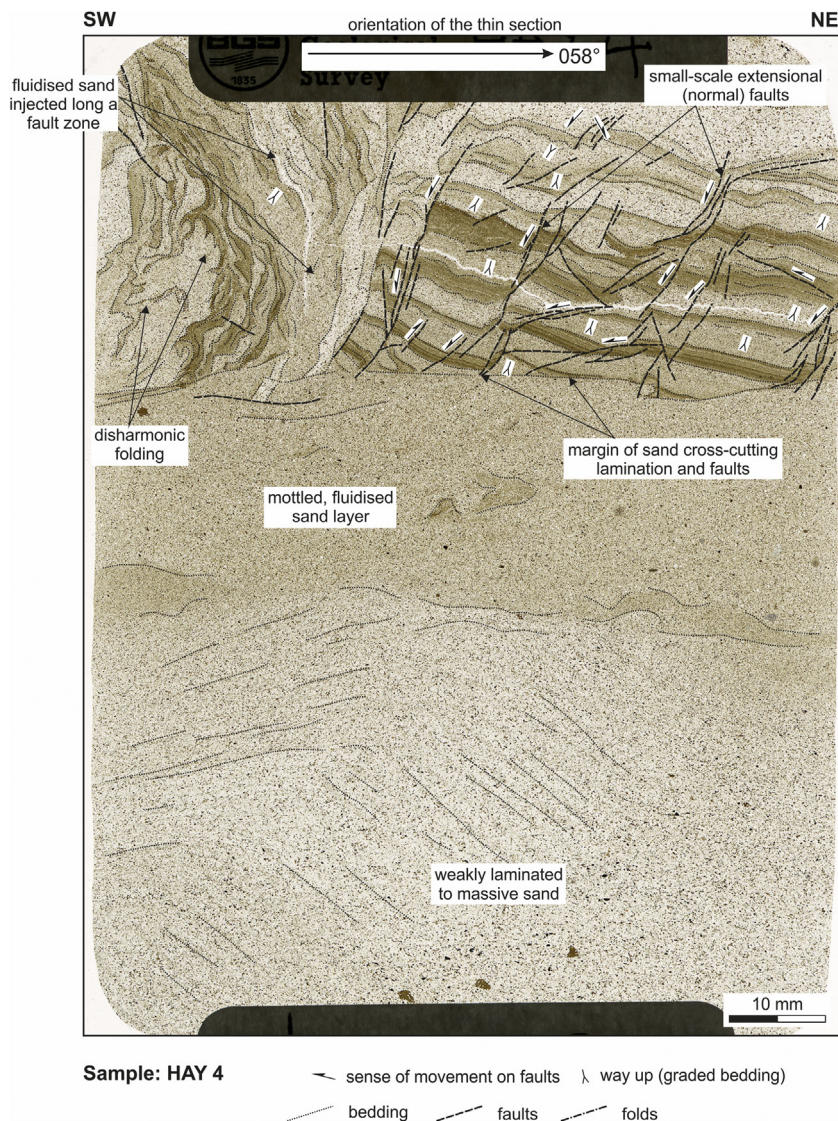


Fig. 16. Annotated high-resolution scan of the large format thin section taken from sample HAY 4 (see text for details). See Figure 12 for details of the location of sample HAY 4.

structurally controlled depression is filled with sediment, any subsequent sand and silt beds will be of uniform thickness until the next phase of movement on the fault and the process starts again. The syndimentary nature of the deformation within the glacialustrine sequence suggests that it was probably deposited on buried glacier ice which was undergoing melt beneath the accumulating sediment pile. The melting of the buried ice would have provided the required accommodation space for the extensional faulting and associated folding which accompanied the localised collapse within glacialustrine sediments.

The glacialustrine sediments either grade upwards, or are conformably overlain (erosive contact; Fig. 8) by coarser-grained glacialuvial sands and gravels. These relationships are consistent with the progressive shallowing of water depths within the proglacial lake and the establishment of a glacialuvial outwash system with the gravels forming transverse bars. Both the glacialuvial and, to a lesser extent, underlying glacialustrine sediments have been folded and thrust (Fig. 7, 8, 10 and 12). The SE-vergence of the folds and comparable sense of displacement on the thrusts are consistent with a direction of ice-push from the N/NW. The folds locally deform earlier developed thrusts, indicative of several phases of thrusting during deformation. However, rather than representing several separate events (i.e. polyphase

deformation), the simplest interpretation is that the folding of the early thrusts occurred as the glacialuvial sediments accommodated an increasing amount of shortening during a single progressive deformation event. This progressive style of deformation is thought to reflect the increasing amounts of shear being transmitted into the sediment pile as the glacier advanced into this former proglacial lake from the N/NW. Although the gravels appear to represent primary (sedimentary) scour-and-fill features, the glacitected contacts clearly represent significant discontinuities within the glacialuvial sequence. The geometry of the folds, coupled with the relatively small displacements (few metres at most) on the sheared/thrust contacts with underlying sands (Figs. 8 and 10) indicate that these detached blocks of gravel have been transported only a relatively short distance towards the E/SE during glacitected.

The glacitected sequence was subsequently incised by a channel-like feature infilled by horizontally stratified, cross-bedded sands and gravels (Fig. 5). These deposits are apparently undeformed, further indicating that incision post-dated glacitected. Both the glacitected sequence and channel deposits are truncated by the “lower” till which was laid down by ice advancing from the NNW. This relationship suggests that glacitected probably occurred in an ice-marginal setting prior

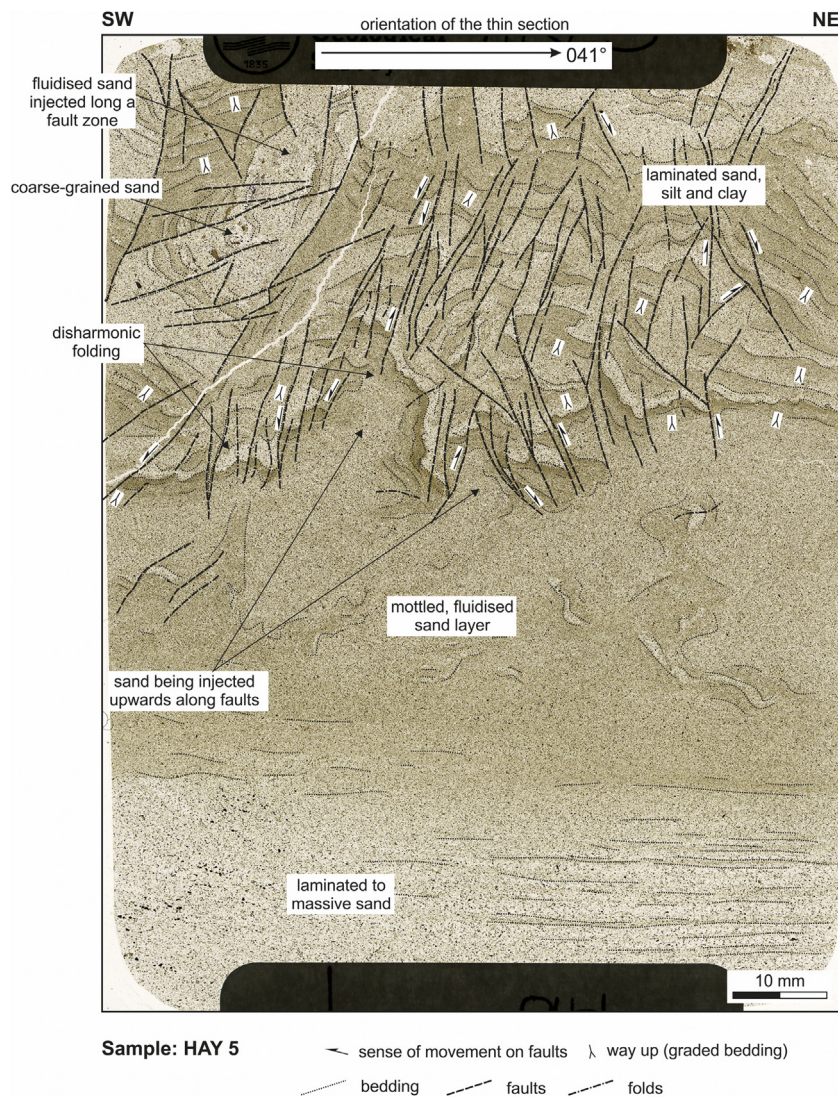


Fig. 17. Annotated high-resolution scan of the large format thin section taken from sample HAY 5 (see text for details). See Figure 12 for details of the location of sample HAY 5.

to the sediments having been overridden by the Teesdale glacier; a conclusion supported by the need for accommodation space to allow the stacking and imbrication of detached thrust-blocks. The phase of incision and deposition of the channel-fill sequence which followed glacitectorism is thought to mark the onset of sedimentation within the Romaldkirk esker, indicating that the Hayberries site had been completely overrun by ice during a significant readvance. Subsequent tunnel closure and shutting down of esker sedimentation is marked by the accretion of the overlying “lower” till which occurred as the overriding ice recoupled with its bed.

The coarsening-upward sequence of planar-bedded sands into cobble to pebble gravel and trough cross-bedded sands and gravels which overlie the “lower” till are interpreted as locally derived ice-proximal deposits which record a relatively minor phase of switching from till to outwash emplacement. These ice-contact tunnel infill sediments were themselves subsequently cannibalized (reworked) during the deposition of the “upper” till which either records a later tunnel closure and recoupling of the ice-bed interface (thereby implying they are essentially canal fills between the two tills, *sensu* Eyles et al., 1982; Clark and Walder, 1994; Evans et al., 1995; Benn and Evans, 1996) or there was a minor oscillation of the glacier margin (implying that the upper Gms lithofacies is proglacial outwash; c.f., Evans et al., 2017, 2018a,b). These

alternative interpretations imply respectively that the Hayberries area has been subject to either: a) a readvance by a Teesdale glacier over lake sediments, followed by subglacial meltwater tunnel excavation, infilling and two ice recoupling/till emplacement events; or b) overriding by at least two readvances of an oscillating ice margin during its overall retreat from the Gueswick Hills moraine assemblage.

6.2. Processes occurring during progressive ice-marginal thrusting

Although the glacitectorism observed at the Hayberries site can be interpreted as having occurred in an ice-marginal setting prior to the glacialacustrine and glacialfluvial sediments having been overridden by ice, the development of the detachments responsible for the thrust-stacking of these sediments is somewhat complex. The thin sections collected from the thrust zones provide valuable insights into the processes occurring during the initial propagation and subsequent evolution of thrusts during the deformation of unconsolidated glacial sequences.

Samples (HAY 3 to 8) collected from the structurally lower thrusts within the glacialacustrine sequence indicate that the relative intensity of folding and disruption caused by the thrusting increases away from the apparent leading edge (propagating tip) of the thrust (see Figs. 12 to 20), towards the direction of ice-push. Detailed

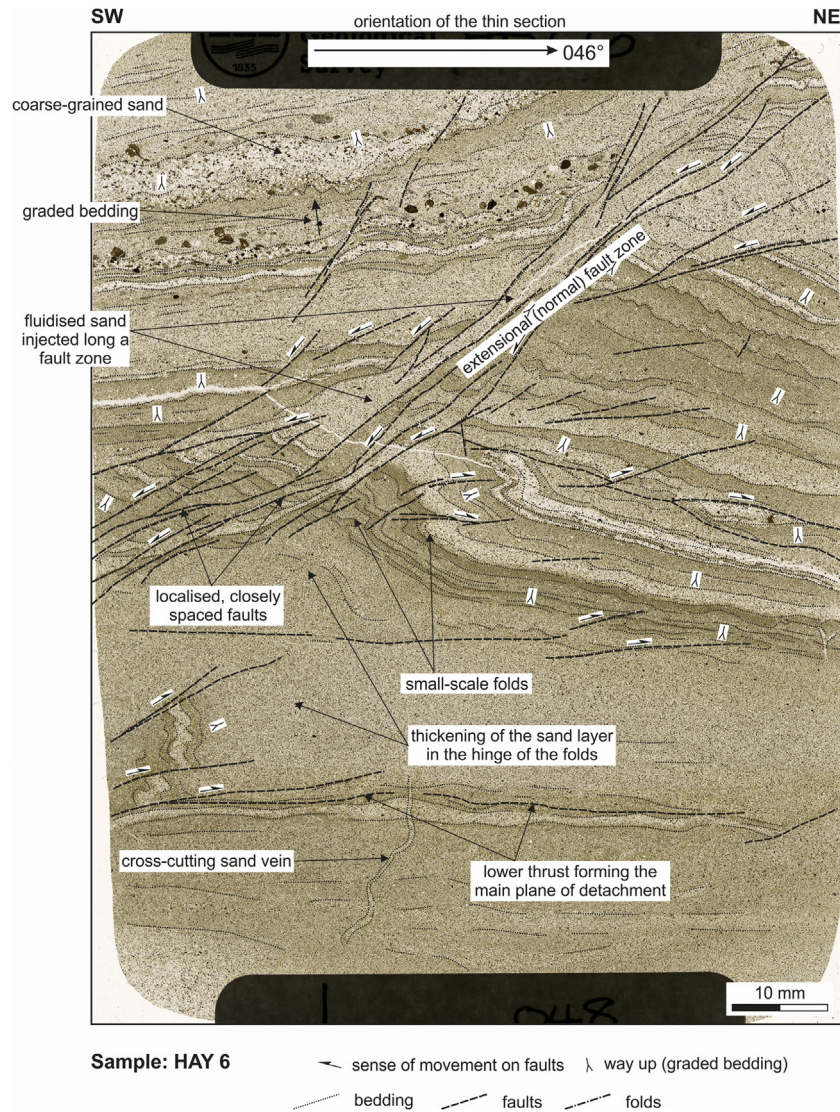


Fig. 18. Annotated high-resolution scan of the large format thin section taken from sample HAY 6 (see text for details). See Figure 12 for details of the location of sample HAY 6.

structural interpretations of the thin sections and their relative position within the thrust zone are shown in Fig. 21. These microstructural maps are combined to produce a detailed schematic microscale cross-section through the thrust-zone (Fig. 22), enabling the changing style of deformation and processes occurring along these thrusts to be examined in detail. The main “basal thrust” to the thrust zone (samples HAY 6, 7 and 8; Fig. 21) occurs at a boundary between the folded and faulted rhythmically laminated sediments in its hanging-wall and the underlying, apparently undeformed massive sands (Fig. 22). This surface would have represented a significant rheological boundary within the deforming pile, initiating thrusting along this lithological contact. Close to the apparent leading edge of the thrust, deformation within the hanging-wall is dominated by asymmetrical E/NE-verging anticlines and synclines, with minor E/NE-directed thrusts cutting the hinges and overturned limbs of the folds (Figs. 21 and 22). The relative intensity of this thrusting increases towards the W/SW (compare samples HAY 7 and 8; Fig. 21), leading to the stacking of several folds (Fig. 22). This is consistent with the increase in the amount of shortening (compression) being accommodated within the hanging-wall of the thrust, away from its propagating tip and towards the direction of ice-push. However, further to the W/SW these small-scale, compressional thrusts within the hanging-wall of the basal thrust appear to have

been reactivated as extensional (normal) faults (e.g., HAY 6; Fig. 21), or are replaced by a complex network of closely spaced subvertical reverse (compressional) faults (e.g., HAY 5; Fig. 21).

The folded and faulted laminated sediments within the hanging-wall and the basal thrust are separated by an apparently laterally extensive (15–25 mm thick) sand layer which thickens within the cores of the anticlines (Figs. 18 and 22). Towards the eastern-end of the thrust zone, the sand is cut by the small-scale thrusts on the hanging-wall (HAY 7 and 8; Fig. 21). However, further away from the leading edge of the thrust zone, the sand becomes increasingly massive with a mottled appearance (HAY 5; Fig. 21). Also in this area, the sand has locally been injected upwards along the brittle faults (e.g. HAY 5 and 6; Fig. 21) and a lithologically similar sand can be observed filling veins, which cut the laminated sediments within the hanging-wall of the thrust (e.g. HAY 7; Fig. 21). Although samples HAY 3 and 4 are from another thrust zone within the glacialacustrine sediments (Fig. 12), they are interpreted as having occupied a structurally more complex position further away from the leading edge of the thrust (see Fig. 22). In these samples the massive to mottled sands clearly cross-cut bedding and the earlier deformation structures and are connected to a more complex funnel-shaped water-escape conduit, which has exploited the pre-existing high-angle

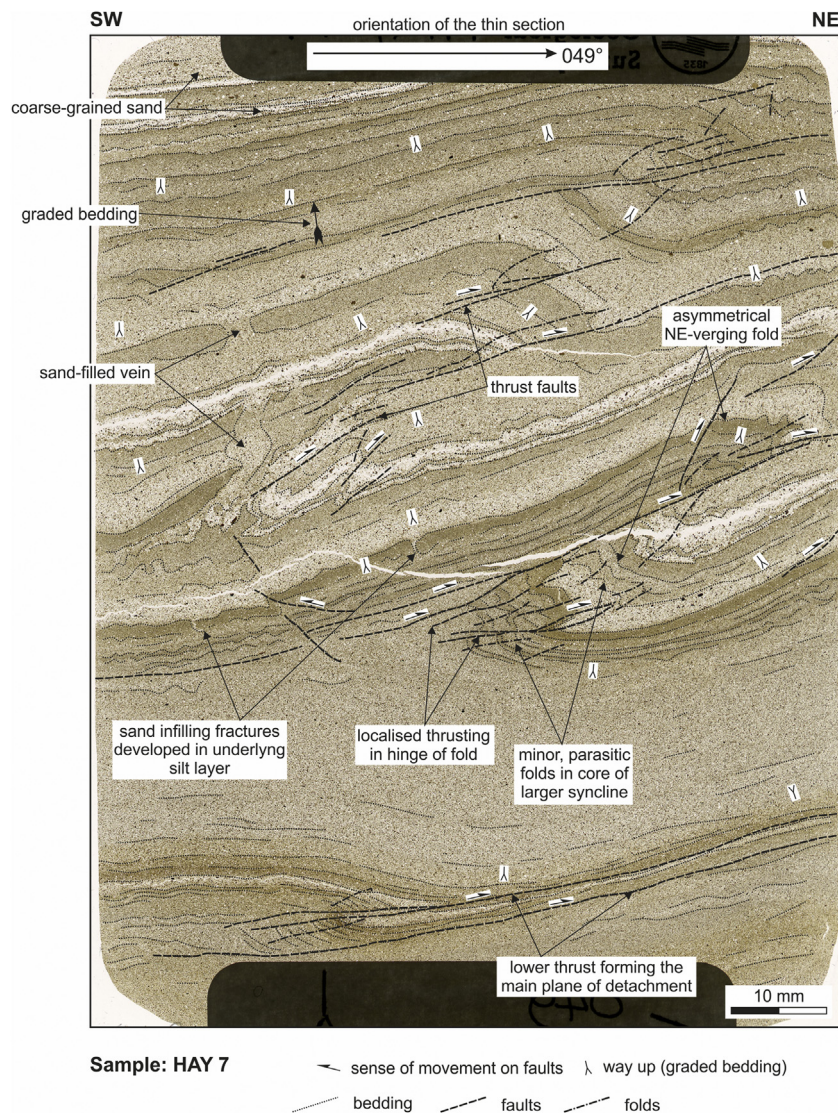


Fig. 19. Annotated high-resolution scan of the large format thin section taken from sample HAY 7 (see text for details). See Figure 12 for details of the location of sample HAY 7.

extensional faults developed within the hanging-wall of the thrust (Fig. 22). The stratified nature of the fill within this water-escape conduit suggests that it accommodated several phases or pulses of fluid flow and probably fed a more extensive network of sand veins (see HAY 3 and 4; Fig. 22).

The relationships outlined above indicate that the main thrusts and small-scale faults acted as fluid pathways, providing a focus for the injection of liquefied sand into the deforming sequence. Furthermore this microtextural evidence suggests that injection occurred during the later stages and may have even largely post-dated deformation. Similar relationships were also observed on the thin sections taken from the thrust within the overlying glacialfluvial sequence (see HAY 1 and 2; Figs. 13 and 14), where initial ductile folding and low-angle faulting was followed by the injection of fluidised sand. Migration of the liquefied sand within the deforming sequence would have resulted in localised increases in sediment volume where the sand was being injected and areas of collapse where it was being removed. These volume changes may have resulted in either the development of new, steeply inclined faults and/or the reactivation of earlier developed thrusts as normal faults. Extensional movement on the normal faults or reactivated thrusts would have facilitated the injection process by opening these structures, assisting the induction of the fluidised sediment. In the

glacialacustrine sediments, the sand layer located immediately above the basal thrust is thought to be the primary source of the remobilised sediment, with liquefaction resulting in the overprinting of bedding and loss of the evidence for thrusting within the sand (Fig. 22).

7. Discussion: implications for thrust propagation during glacitectonic deformation

Macroscale analysis of the deformation structures exposed within the Hayberries quarry indicate that glacitectonism of glacialacustrine and glacialfluvial sequences occurred in response to the E/SE-directed ice advance. The folding and thrust stacking of the glacialfluvial sands and gravel occurred in an ice-marginal setting prior to the overriding of the sequence by the lobate front of the Teesdale glacier. Glacitectonism may have occurred shortly after the filling of the proglacial lake by the coarsening upwards sequence of sands, silts and clays, followed by the deposition of the ice-proximal, glacialfluvial sands and gravels. If this relative chronology of events is correct then the sediments being deformed by the approaching Teesdale glacier may have still been relatively water-rich.

A number of published studies have argued that elevated water pressures can have a significant effect of glacitectonic deformation by either leading to the pervasive weakening of the sediment pile

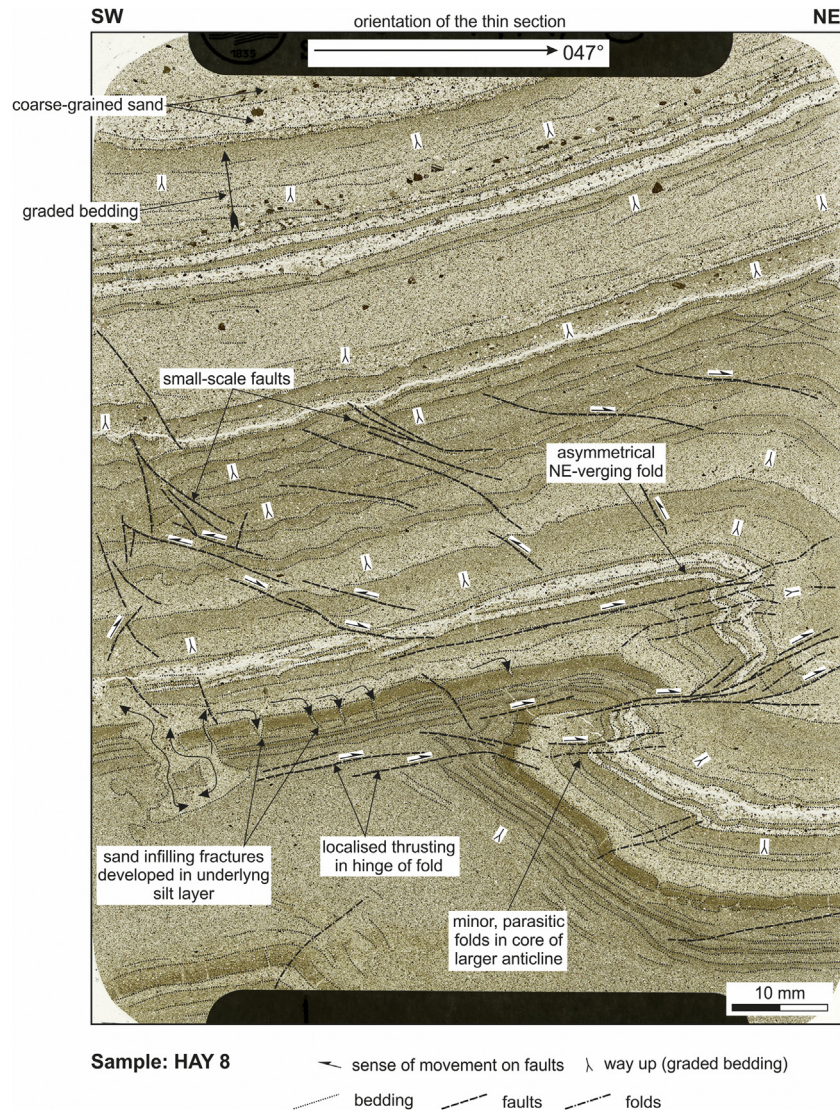


Fig. 20. Annotated high-resolution scan of the large format thin section taken from sample HAY 8 (see text for details). See Figure 12 for details of the location of sample HAY 8.

or the focusing of deformation along discrete, water-lubricated detachments (Alley, 1989a,b; Fischer and Clarke, 2001; Kjær et al., 2006; Phillips and Merritt, 2008). The development of low-friction, water-lubricated detachments (thrusts) is thought to have a considerable effect on the style and magnitude of glacitectonics, not only facilitating the transport of large thrust-blocks of sediment and/or bedrock (Phillips and Merritt, 2008; Burke et al., 2009; Vaughan-Hirsch et al., 2013; Aber and Ber, 2007; Andreassen et al., 2007; Rütger et al., 2013; Sigfusdottir et al., 2019), but also the construction of large thrust-block or composite moraines (Croot, 1987; Bennett, 2001; Pedersen, 2005; Aber and Ber, 2007; Benediktsson et al., 2008; Vaughan-Hirsch and Phillips, 2017; Phillips et al., 2017; Sigfusdottir et al., 2018; 2019). Several studies have suggested that increased porewater-pressure within ice-marginal to proglacial sediments are likely to occur due to normal loading by ice and tectonic thickening, as well as the basal shear stress applied by the advancing glacier (van der Wateren, 1985; Phillips and Merritt, 2008; Vaughan-Hirsch and Phillips, 2017; Sigfusdottir et al., 2019). For example, Vaughan-Hirsch and Phillips (2017) argued that the migration of pressurised groundwater through a laterally extensive sand sheet within the mud-rich Aberdeen Ground Formation (North Sea) facilitated the

development of the décollement at the base of a c. 90–100 m thick, forward-propagating imbricate thrust-stack. In this conceptual model, loading of the sediments by a major ice sheet led to an increase in groundwater pressures and the development of significant hydrostatic gradient driving the migration of water from beneath the ice out into its foreland. Vaughan-Hirsch and Phillips (2017) suggested that the resultant “pressure wave” within the glacier bed migrates in front of the advancing ice margin, lowering the cohesive strength of the permeable sand, leading to failure, and the propagation of a water-lubricated, bedding-parallel detachment.

The glacitectonic deformation at Hayberries is, by comparison, on a much smaller scale and apparently did not lead to the formation of a significant thrust-block moraine. However, both macro- and microstructural evidence seen at this site indicate that the introduction of pressurised meltwater into the deforming sediment pile did occur during glacitectonism and that it had an effect on the development of the thrusts. Similar microtextural relationships supporting the injection of liquefied sediment during thrusting has been recently described by Sigfusdottir et al. (2019) from detachments developed within two glacitectonic complexes exposed at Melasveit, western Iceland. Evidence from the

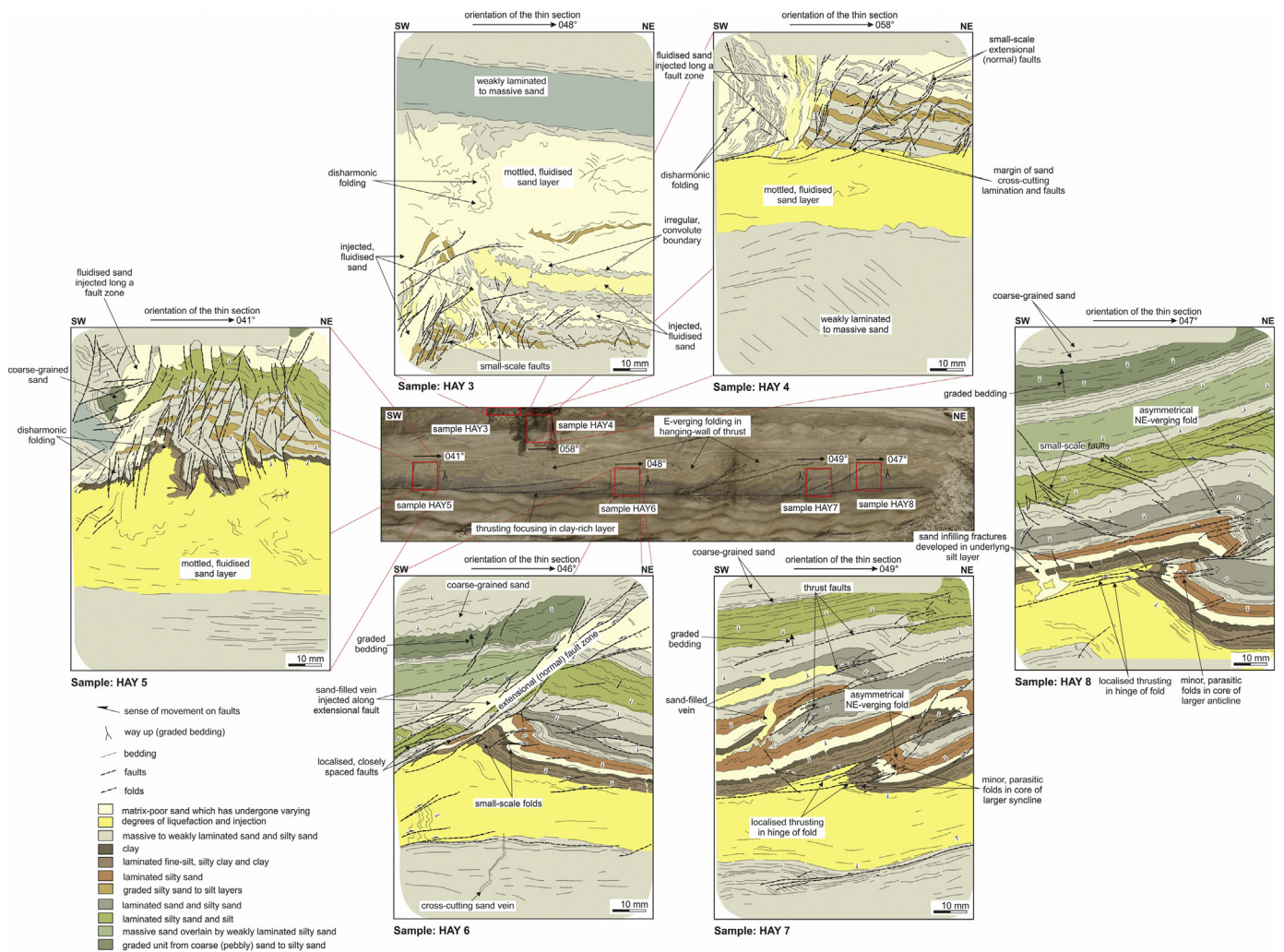


Fig. 21. Detailed micromorphological and microstructural interpretations of thin sections HAY 3–8 and their position within the low-angle thrust deforming the thinly bedded glacialacustrine sediments. The colours represent the different sand, silt and clay units identified in thin section and their correlation between the samples. The yellow colours represent fine grained sand which has undergone varying degrees of liquefaction, remobilisation and injection (see text for details).

Hayberries site indicates that the main thrusts and small-scale faults acted as fluid pathways, providing a focus for the injection of liquefied sand into the deforming sequence. However, the thin sections reveal that the relative intensity of liquefaction and injection of the sand increases away from the leading edge of these detachments (see Fig. 22).

Microtextural evidence suggests that injection of the mobilised sand occurred during the later stages of glacial tectonic deformation. Close to the propagating tip of the thrusts, deformation within their hanging-walls was initially ductile (folding), followed by small-scale brittle thrusting and imbrication as the laminated sands, silts and clays accommodated increasing amounts of shortening. The apparently limited number of sand veins (see HAY 7 and 8; Fig. 21) within this part of the thrust zone suggests it may have been relatively “dry”. Modelling carried out by Brenner and Guðmundsson (2004) on hydrofracture systems shows that fluid overpressure varies linearly from a maximum at the centre of the fracture, to zero at its propagating tip. The fluid front, marking the leading edge of water penetration into the evolving hydrofracture, may coincide with the fracture tip. However, where fracture propagation is facilitated by the presence of a pre-existing plane of weakness, the hydrofracture may propagate in advance of this front, with a

‘dry zone’ between the fluid front and fracture tip. If this model is applied to the Hayberries thrust zones then the propagation of these glacial tectonic detachments may have been driven by an increase in porewater pressures in the more permeable layers within the sediment pile as a result of loading by the advancing Teesdale glacier. In the glacialacustrine sediments, pressurised water would have been confined within sand layers by the less permeable laminated silts and clays. The bedding-parallel nature of the thrusts clearly indicates that they were exploiting this pre-existing plane of weakness. Consequently, a ‘dry zone’ may have existed between the propagating tip of the thrust and the fluid front, which subsequently migrated along this detachment.

Experimental data suggests that the structural style and geometric characteristics of a developing thrust-complex above its basal décollement are strongly controlled by the frictional properties of the sequence beneath this surface (Davis et al., 1984; Nieuwland et al., 2000). The potential introduction of pressurised water into the sand layers within the Hayberries glacialacustrine sequence would have lowered its cohesive strength and, if the water pressures were high enough, led to the development of a low-friction layer within the thrust zone. This would not only have assisted thrust propagation (c.f. van Gijssel, 1987; Andersen et al., 2005), but also the transport of the detached blocks of sediment. Prior to the introduction of the

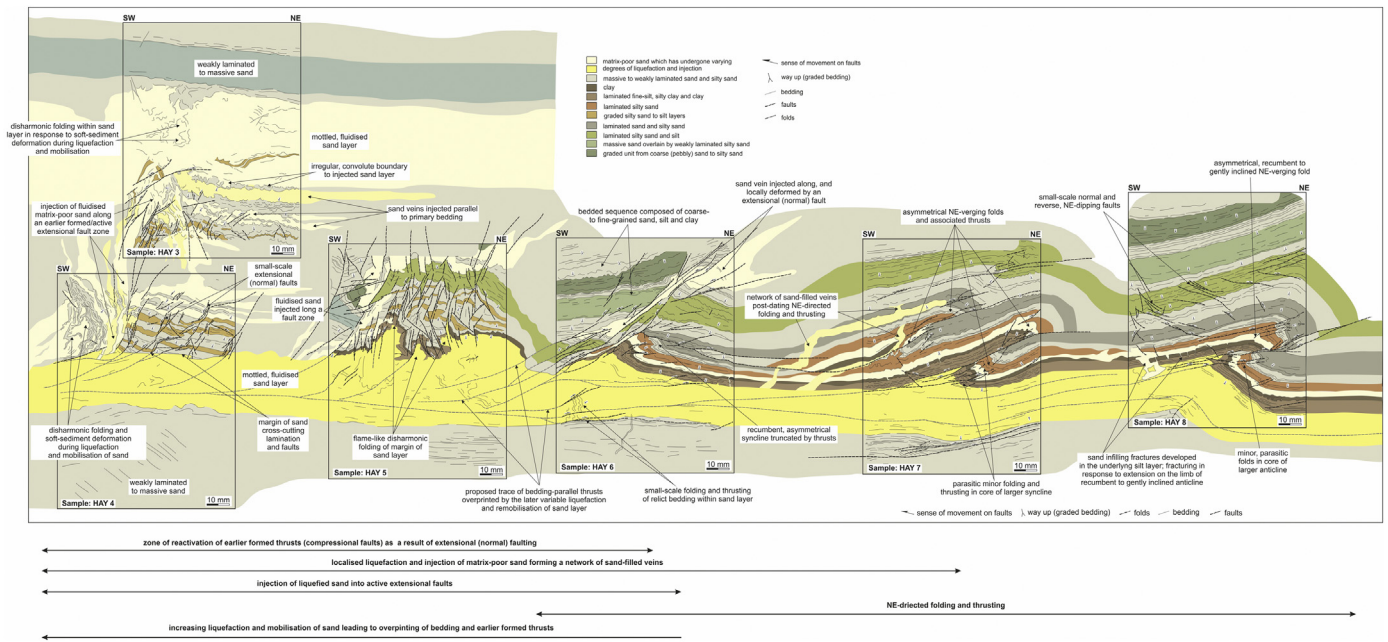


Fig. 22. Conceptual model of the processes occurring within a low-angle thrust based upon the detailed micromorphological and microstructural interpretation of the large format thin sections. The model highlights the changing style of deformation along the thrust and the increased evidence of liquefaction, remobilisation and injection of the fine-grained sands at a deep structural level within the thrust zone (see text for details).

pressurised water, the relatively higher-frictional “dry zone” may have promoted folding and thrusting, and the detachment of short, moderately inclined thrust nappes within the hanging-wall as the sediments accommodated ice-push. However, once the fluid front had penetrated the evolving thrust, the cohesive strength of the sand would have lowered dramatically leading to thrust-sheet gliding (Davis et al., 1984; Nieuwland et al., 2000), decoupling along the thrust plane, with the potential for the detachment of longer slabs of sediment effectively switching off deformation in the hanging-wall. Consequently, the frictional properties of the sediments within the thrusts at Hayberries would have changed from high-frictional sand to a low-friction substrate by the simple addition of pressurised meltwater. Increase water pressure also resulted in localised liquefaction and remobilisation of the sediment, with the lateral migration of this fluidised sand resulting in localised collapse and extensional (normal) faulting. Escape of this pressurised water-sediment mix along pre-existing faults would have led to the lowering of water pressure within the thrust zone. This may have effectively switched off deformation and movement along the thrust or the development of a stick-slip style of motion on these glaciectonic detachments.

8. Conclusions

The results of the detailed macro- and microscale sedimentological and structural study of the Quaternary sediments exposed at Hayberries Quarry, Teesdale, County Durham (UK) presented here contribute to our understanding of the progressive deformation of glacial sequences, and the role played by water during the detachment and transport of sediment blocks during ice-marginal glaciectonic thrusting. The sediments record a sequence of depositional environments commencing with the formation of a proglacial lake which accommodated the deposition of coarsening-upwards sequence of rhythmically laminated sands, silts and clays. The occurrence of dropstones within the upper most part of this glacial sequence may record the increasing proximity of the ice margin and/or increased bergs calving into the lake. Synsedimentary normal faulting within the glacial sequence suggests that it was probably deposited on buried glacier

ice which was undergoing melting beneath the accumulating sediment pile, thereby providing the required accommodation space for the extensional faulting and localised collapse within glacialustrine sediments.

The glacialustrine sediments are conformably overlain by glacialuvial sands and gravels, which record the shallowing of the lake and the establishment of a glacialuvial outwash system. This glacialuvial sequence is folded and thrust with the geometry of these deformation structures being consistent with glaciectonism having occurred in an ice-marginal setting in response to ice-push from the N/NW, prior to the Hayberries site being overridden by the Teesdale glacier. The simplest interpretation of the macroscale relationships between the ductile folds and brittle thrusts is that deformation occurred during a single progressive event as the glacialuvial sediments accommodated an increasing amount of shortening imposed by the advancing lobate ice margin. Detailed microstructural analysis reveals that initial folding and thrusting within the hanging-walls of the thrusts was followed by the injection of fluidised sand along the developing thrust planes. It is argued that the introduction of pressurised meltwater and sediment along these structures would have facilitated decoupling and enhanced displacement along these detachments as a result of thrust gliding.

Glaciectonism at Hayberries was followed by a phase of incision and deposition of the channel-fill sequence marking the onset of sedimentation within the Romalldkirk esker. Furthermore this indicates that the Hayberries site had been completely overrun by ice during a significant readvance. Subsequent tunnel closure and shutting down of esker sedimentation is marked by the accretion of the upper till which was laid down as the overriding ice recoupled with its bed.

Acknowledgements

The authors would like to thank Durham County Council for granting access to work in the Hayberries Quarry. Although abandoned, the quarry is managed for its wildlife, especially

ground nesting birds, by the Countryside Service, Durham County Council and therefore permission must be sought before gaining access. Dave Bridgland (Durham University) kindly identified the clast lithologies. Andrew Finlayson is thank for his constructive comments on an earlier version of this paper. The two anonymous reviewers are thanked for their positive and constructive reviews. Emrys Phillips publishes with permission of the Chief Executive of the British Geological Survey.

Appendix A. Supplementary data

Supplementary data associated with this article can be found, in the online version, at <https://doi.org/10.1016/j.pgeola.2019.08.001>.

References

- Aber, J.S., Ber, A., 2007. Glaciotectionism. *Developments in Quaternary Science* 6. Elsevier, Amsterdam.
- Alley, R.B., 1989a. Water pressure coupling of sliding and bed deformation: 1. Water system. *Journal of Glaciology* 35, 108–118.
- Alley, R.B., 1989b. Water pressure coupling of sliding and bed deformation: II. Velocity-depth profiles. *Journal of Glaciology* 35, 119–129.
- Andersen, L.T., Hansen, D.L., Huse, M., 2005. Numerical modelling of thrust structures in unconsolidated sediments: implications for glaciotectionic deformation. *Journal of Structural Geology* 27, 587–596.
- Andreassen, K., Ødegaard, C.M., Rafalsen, B., 2007. Imprints of former ice streams, imaged and interpreted using industry three-dimensional seismic data from the south-western Barents Sea, vol. 277. Geological Society, London, pp. 151–169. doi:<http://dx.doi.org/10.1144/gsl.sp.2007.277.01.09> Special Publications.
- Baroni, C., Fasano, F., 2006. Micromorphological evidence of warm-based glacier deposition from the Ricker Hills Tillite (Victoria Land, Antarctica). *Quaternary Science Reviews* 25, 976–992.
- Benediktsson, Í.Ö., Möller, P., Ingólfsson, Ó., van der Meer, J.J.M., Kjær, K.H., Krüger, J., 2008. Instantaneous end moraine and sediment wedge formation during the 1890 glacier surge of Brúarjökull, Iceland. *Quaternary Science Reviews* 27, 209–234. doi:<http://dx.doi.org/10.1016/j.quascirev.2007.10.007>.
- Benn, D.I., 1994. Fluted moraine formation and till genesis below a temperate glacier: Slettmarkbreen, Jotunheimen, Norway. *Sedimentology* 41, 279–292.
- Benn, D.I., Ballantyne, C.K., 1994. Reconstructing the transport history of glaciogenic sediments: a new approach based on the co-variance of clast form indices. *Sedimentary Geology* 91, 215–227.
- Benn, D.I., Evans, D.J.A., 1996. The interpretation and classification of subglacially-deformed materials. *Quaternary Science Reviews* 15, 23–52.
- Bennett, M.R., 2001. The morphology, structural evolution and significance of push moraines. *Earth-Science Reviews* 53, 197–236. doi:[http://dx.doi.org/10.1016/S0012-8252\(00\)00039-8](http://dx.doi.org/10.1016/S0012-8252(00)00039-8).
- Brenner, S.L., Gudmundsson, A., 2004. Arrest and aperture variation of hydrofractures in layered reservoirs. In: Cosgrove, J.W., Engelder, T. (Eds.), *The Initiation, Propagation and Arrest of Joints and Other Fractures*, vol. 231. Geological Society, London, pp. 117–128 Special Publications.
- Brumme, J., 2015. Three-dimensional microfabric analyses of Pleistocene tills from the cliff section Dwasieden on Rügen (Baltic Sea coast): micromorphological evidence for subglacial polyphase deformation (PhD thesis). Ernst-Moritz-Arndt-Universität, Greifswald, pp. 210pp.
- Burke, H., Phillips, E., Lee, J.R., Wilkinson, I.P., 2009. Imbricate thrust stack model for the formation of glaciotectionic rafts: an example from the Middle Pleistocene of north Norfolk, UK. *Boreas* 38, 620–637.
- Clark, P.U., Walder, J.S., 1994. Subglacial drainage, eskers, and deforming beds beneath the Laurentide and Eurasian ice sheets. *Bulletin of the Geological Society of America* 106, 304–314.
- Croot, D.G., 1987. Glacio-tectonic structures: a mesoscale model of thin-skinned thrust sheets? *Journal of Structural Geology* 9, 797–808. doi:[http://dx.doi.org/10.1016/0191-8141\(87\)90081-2](http://dx.doi.org/10.1016/0191-8141(87)90081-2).
- Davis, D., Suppe, J., Dahlen, F.A., 1984. Mechanics of fold-and-thrust belts and accretionary wedges: Cohesive Coulomb theory. *Journal of Geophysical Research* 89, 10087–10101.
- Evans, D.J.A., Benn, D.I., 2004. A practical guide to the study of glacial sediments. Arnold, London.
- Evans, D.J.A., Hiemstra, J.F., 2005. Till deposition by glacier submarginal, incremental thickening. *Earth Surface Processes and Landforms* 30, 1633–1662.
- Evans, D.J.A., Phillips, E.R., Hiemstra, J.F., Auton, C.A., 2006. Subglacial till: formation, sedimentary characteristics and classification. *Earth Science Reviews* 78, 115–176.
- Evans, D.J.A., Roberts, D.H., Evans, S.C., 2016. Multiple subglacial till deposition: a modern exemplar for Quaternary palaeoglaciology. *Quaternary Science Reviews* 145, 183–203.
- Evans, D.J.A., Phillips, E.R., Dinnage, M., 2017. Glacifluvial landforms of the Romaldkirk/Egglesstone area and their relationship to the Gueswick Hills moraine assemblage. In: Evans, D.J.A. (Ed.), *The Quaternary landscape history of Teesdale and the North Pennines – Field Guide*. Quaternary Research Association, London, pp. 158–183.
- Evans, D.J.A., Dinnage, M., Roberts, D.H., 2018a. Glacial geomorphology of Teesdale, northern Pennines, England: Implications for upland styles of Ice stream operation and deglaciation in the British-Irish Ice Sheet. *Proceedings of the Geologists' Association* 129, 697–735.
- Evans, D.J.A., Roberts, D.H., Hiemstra, J.F., Nye, K.M., Wright, H., Steer, A., 2018b. Submarginal debris transport and till formation in active temperate glacier systems: The southeast Iceland type locality. *Quaternary Science Reviews* 195, 72–108.
- Evans, D.J.A., 2018. *Till: A Glacial Process Sedimentology*. John Wiley and Sons Ltd, UK.
- Eyles, N., Sladen, J.A., Gilroy, S., 1982. A depositional model for stratigraphic complexes and facies superimposition in lodgement tills. *Boreas* 11, 317–333.
- Fischer, U.H., Clarke, G.K.C., 2001. Review of subglacial hydro-mechanical coupling: Trapridge Glacier, Yukon Territory, Canada. *Quaternary International* 86, 29–43. doi:[http://dx.doi.org/10.1016/S1040-6182\(01\)00049-0](http://dx.doi.org/10.1016/S1040-6182(01)00049-0).
- Gehrmann, A., Hüneke, H., Meschede, M., Phillips, E., 2017. 3D microstructural architecture of deformed glaciogenic sediments associated with large-scale glaciotectionism, Jasmund Peninsula (NE Rügen), Germany. *Journal of Quaternary Science* 32, 213–230. doi:<http://dx.doi.org/10.1002/jqs.2843>.
- Hart, J., Rose, J., 2001. Approaches to the study of glacier bed deformation. *Quaternary International* 86, 45–58.
- Hiemstra, J.F., Rijdsdijk, K.F., 2003. Observing artificially induced strain: implications for subglacial deformation. *Journal of Quaternary Science* 18, 373–383.
- Hooyer, T.S., Iverson, N.R., 2000. Diffusive mixing between shearing granular layers: constraints on bed deformation from till contacts. *Journal of Glaciology* 46, 641–651.
- Ildefonse, B., Mancktelow, N.S., 1993. Deformation around rigid particles: the influence of slip at the particle/matrix interface. *Tectonophysics* 221, 345–359.
- Khatwa, A., Tulaczyk, S., 2001. Microstructural interpretations of modern and Pleistocene subglacially deformed sediments: the relative role of parent material and subglacial processes. *Journal of Quaternary Science* 16, 507–517.
- Kjær, K.H., Larsen, E., van der Meer, J.J.M., Ingólfsson, Ó., Krüger, J., Benediktsson, I.O., Knudsen, C.G., Schomacker, A., 2006. Subglacial decoupling at the sediment/bedrock interface: a new mechanism for rapid flowing ice. *Quaternary Science Reviews* 25, 2704–2712.
- Lukas, S., Benn, D.I., Boston, C.M., Brook, M., Coray, S., Evans, D.J.A., Graf, A., Kellerer-Pirklbauer, A., Kirkbride, M.P., Krabbendam, M., Lovell, H., Machiedo, M., Mills, S. C., Nye, K., Reinardy, B.T.I., Ross, F.H., Signer, M., 2013. Clast shape analysis and clast transport paths in glacial environments: a critical review of methods and the role of lithology. *Earth-Science Reviews* 121, 96–116.
- March, A., 1932. *Mathematische Theorie der Regelung nach der Korngestalt bei affiner Deformation*. Zeitschrift für Kristallographie 81, 285–297.
- Menzies, J., 2000. Micromorphological analyses of microfibrils and microstructures indicative of deformation processes in glacial sediments. In: Maltman, A.J., Hubbard, B., Hambrey, M.J. (Eds.), *Deformation of glacial materials*, vol. 176. Geological Society, London, pp. 245–257 Special Publication.
- Menzies, J., van der Meer, J.J.M., Rose, J., 2006. Till – a glacial “tectomict”, a microscopic examination of a till’s internal architecture. *Geomorphology* 75, 172–200.
- Miall, A.D., 1977. A review of the braided river depositional environment. *Earth Science Reviews* 13, 1–62.
- Miall, A.D., 1978. Lithofacies types and vertical profile models in braided rivers: a summary. In: Miall, A.D. (Ed.), *Fluvial Sedimentology*, vol. 5. *Geology Memoir*, pp. 597–604.
- Mills, D.A.C., Hull, J.H., 1976. *Geology of the country around Barnard Castle*. Memoir of the Geological Survey of Great Britain.
- Nieuwland, D.A., Leutscher, J.H., Gast, J., 2000. Wedge equilibrium in fold-and-thrust belts: prediction of out-of-sequence thrusting based on sandbox experiments and natural examples. *Geologie en Mijnbouw* 79, 81–91.
- Pedersen, S.A.S., 2005. Structural analysis of the Rubjerg Knude Glaciotectionic Complex, Vendsyssel, northern Denmark. Copenhagen.
- Passchier, C.W., Trouw, R.A.J., 1996. *Microtectonics*. Springer.
- Phillips, E., Merritt, J.W., Auton, C.A., Golledge, N.R., 2007. Microstructures developed in subglacially and proglacially deformed sediments: faults, folds and fabrics, and the influence of water on the style of deformation. *Quaternary Science Reviews* 26, 1499–1528.
- Phillips, E.R., Auton, C.A., 2000. Micromorphological evidence for polyphase deformation of glaciolacustrine sediments from Strathspey, Scotland. In: Maltman, A.J., Hubbard, B., Hambrey, M.J. (Eds.), *Deformation of glacial materials*, vol. 176. Geological Society, London, pp. 279–291 Special Publication.
- Phillips, E., Merritt, J., 2008. Evidence for multiphase water-escape during rafting of shelly marine sediments at Clava, Inverness-shire, NE Scotland. *Quaternary Science Reviews* 27, 988–1011.
- Phillips, E., Lee, J.R., 2011a. Description, measurement and analysis of glaciotectionically deformed sequences. In: Phillips, E., Lee, J.R., Evans, H.M. (Eds.), *Glaciotectionics: Field Guide*. Quaternary Research Association ISBN 0 907 780 830.
- Phillips, E.R., van der Meer, J.J.M., Ferguson, A., 2011b. A new ‘microstructural mapping’ methodology for the identification and analysis of microfibrils within glacial sediments. *Quaternary Science Reviews* 30, 2570–2596.
- Phillips, E.R., Lipka, E., van der Meer, J.J.M., 2013a. Micromorphological evidence of liquefaction and sediment deposition during basal sliding of glaciers. *Quaternary Science Reviews* 81, 114–137.
- Phillips, E., Everest, J., Reeves, H., 2013b. Micromorphological evidence for subglacial multiphase sedimentation and deformation during overpressurized fluid flow associated with hydrofracturing. *Boreas* 42, 395–427.

- Phillips, E., Evans, D.J.A., Atkinson, N., Kendall, A., 2017. Structural architecture and glaciectonic evolution of the Mud Buttes cupola hill complex, southern Alberta, Canada. *Quaternary Science Reviews* 164, 110–139.
- Phillips, E., Evans, D.J.A., van der Meer, J.J.M., Lee, J.R., 2018a. Microscale evidence of liquefaction and its potential triggers during soft-bed deformation within subglacial traction tills. *Quaternary Science Reviews* 181, 123–143.
- Phillips, E., Spagnolo, M., Alasdair, C.J., Pilmer, A.C.J., Rea, B.R., Piotrowski, J.A., Ely, J. C., Carr, S., 2018b. Progressive ductile shearing during till accretion within the deforming bed of a palaeo-ice stream. *Quaternary Science Reviews* 193, 1–23.
- Rijsdijk, K.F., Owen, G., Warren, W.P., McCarroll, D., van der Meer, J.J.M., 1999. Clastic dykes in over-consolidated tills: evidence for subglacial hydrofracturing at Killiney Bay, eastern Ireland. *Sedimentary Geology* 129, 111–126.
- Rüther, D.C., Andreassen, K., Spagnolo, M., 2013. Aligned glaciectonic rafts on the central Barents Sea seafloor revealing extensive glaciectonic erosion during the last deglaciation. *Geophysical Research Letters* 40, 6351–6355. doi:<http://dx.doi.org/10.1002/2013GL058413>.
- Sigfusdottir, T., Benediktsson, I.O., Phillips, E., 2018. Active retreat of a Late Weichselian marine-terminating glacier: an example from Melasveit, western Iceland. *Boreas* doi:<http://dx.doi.org/10.1111/bor.12306>.
- Sigfusdottir, T., Phillips, E., Benediktsson, I.O., 2019. The role of pressurised water in large-scale glaciectonic thrusting: Evidence from submarine, ice-marginal thrust-block moraines in Melasveit, W-Iceland. *Quaternary Research*.
- van Gijssel, K., 1987. A lithostratigraphic and glaciectonic reconstruction of the Lamstedt Moraine, Lower Saxony (FRG). In: van der Meer, J.J.M. (Ed.), *Tills and Glaciectonics*. A.A. Balkema, Rotterdam, pp. 145–156.
- van der Meer, J.J.M., 1987. Micromorphology of glacial sediments as a tool in distinguishing genetic varieties of till. *Geological Survey of Finland Special Paper* 3, 77–89.
- van der Meer, J.J.M., 1993. Microscopic evidence of subglacial deformation. *Quaternary Science Reviews* 12, 553–587.
- van der Meer, J.J.M., Laban, C., 1990. Micromorphology of some North Sea till samples, a pilot study. *Journal of Quaternary Science* 5, 95–101.
- van der Meer, J.J.M., Rabassa, J.O., Evenson, E.B., 1992. Micromorphological aspects of glaciolacustrine sediments in northern Patagonia, Argentina. *Journal of Quaternary Science* 7, 31–44.
- van der Meer, J.J.M., Verbers, A.L.L.M., 1994. The micromorphological character of the Ballycraheen Formation (Irish Sea Till): a first assessment. In: Warren, Croot (Ed.), *Formation and Deformation of Glacial Deposits*. Balkema, Rotterdam, pp. 39–49.
- van der Meer, J.J.M., Menzies, J., Rose, J., 2003. Subglacial till, the deformable glacier bed. *Quaternary Science Reviews* 22, 1659–1685.
- van der Meer, J.J.M., Kjaer, K., Krüger, J., 1999. Subglacial water escape structures and till structure, Sléttjökull, Iceland. *Journal of Quaternary Science* 14, 191–415.
- van der Meer, J.J.M., Kjær, K.H., Krüger, J., Rabassa, J., Kilfeather, A.A., 2009. Under pressure: clastic dykes in glacial settings. *Quaternary Science Reviews* 28, 708–720.
- van der Wateren, D.F.M., 1985. A Model of Glacial Tectonics, Applied to the Ice-pushed Ridges in the Central Netherlands, vol. 34. Geological Society of Denmark, Bulletin, pp. 55–74.
- van der Wateren, F.M., 1995. Process of glaciectonism. In: Menzies, J. (Ed.), *Glacial Environments. Modern Glacial Environments: Processes, Dynamics and Sediments*, vol. 1. Butterworth-Heinemann, Oxford, pp. 309–335.
- van der Wateren, F.M., Kluiving, S.J., Bartek, L.R., 2000. Kinematic indicators of subglacial shearing. In: Maltman, A.J., Hubbard, B., Hambrey, M.J. (Eds.), *Deformation of glacial materials*, vol. 176. Geological Society, London, pp. 259–278 Special Publications.
- Vaughan-Hirsch, D.P., Phillips, E.R., 2017. Mid-Pleistocene thin-skinned glaciectonic thrusting of the Aberdeen Ground Formation, Central Graben region, central North Sea. *Journal of Quaternary Science* 32, 196–212. doi:<http://dx.doi.org/10.1002/jqs.2836>.
- Vaughan-Hirsch, D.P., Phillips, E., Lee, J.R., Hart, J.K., 2013. Micromorphological analysis of poly-phase deformation associated with the transport and emplacement of glaciectonic rafts at West Runton, north Norfolk, UK. *Boreas* 42, 376–394.